AD NUMBER

AD872306

NEW LIMITATION CHANGE

TO

Approved for public release, distribution
unlimited

FROM

Distribution authorized to U.S. Gov't.
agencies and their contractors; Critical
Technology; Jul 1970. Other requests shall
be referred to National Aeronautics and
Space Administration, Attn: JPL, Pasadena,
CA.

AUTHORITY

USANWC ltr, 30 Aug 1974

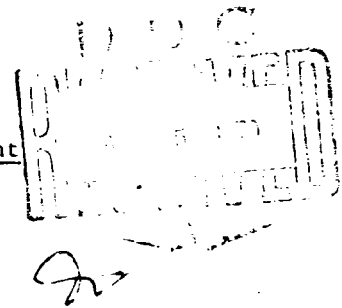# THERMAL ANALYSES STUDIES ON CANDIDATE SOLID JPL PROPELLANTS FOR HEAT STERILIZABLE MOTORS

by

Jack M. Pakulak, Jr.
and
Edward Kuletz
Propulsion Development Department

ABSTRACT.   Times to deflagration of solid JPL propellant grains varying in size and geometry have been measured, and the results have been analyzed in light of the thermal explosion theory.   In addition, laboratory-scale thermoanalytical techniques have been used to study the procedural chemical kinetics of the decomposition reactions of representative solid JPL propellants.   The results of these studies indicate that, for the propellants considered, estimates of thermal deflagration times can be made on the basis of laboratory-scale experiments.   The effects of sterilization heat cycling tests on solid JPL propellant grains varying in size and geometry have also been studied and the results are herein reported.

NAVAL WEAPONS CENTER

CHINA LAKE, CALIFORNIA ● JULY 1970

NAVAL WEAPONS CENTER
AN ACTIVITY OF THE NAVAL MATERIAL COMMAND

FOREWORD

The study described in this report was undertaken as a result of a request by the Jet Propulsion Laboratory to the U. S. Naval Ordnance Test Station (now Naval Weapons Center) via letter SMu-31 of 14 December 1965. They were concerned about the potential thermal hazard or "cook-off" problem during the heat sterilization of solid propellant grains.

This study was supported by JPL Purchase Order Nos. Z-351290 (propellant degradation studies) and Z-351291 (heat sterilization tests).

As requested by the Jet Propulsion Laboratory, the original manuscript was reviewed for technical accuracy by Dr. Joseph Wenograd of the University of Hartford, West Hartford, Connecticut. The revised manuscript was reviewed for technical accuracy by Warren W. Oshel.

ii

CONTENTS

INTRODUCTION

The adoption of sterilization requirements for spacecraft designed to land on extra-terrestrial bodies has necessitated significant re-evaluations of specifications regarding thermal cycling. In the area of solid propellant technology it has been necessary to formulate propellants with sufficient thermal stability to withstand repeated and prolonged exposures to temperatures as high as 135°C. Propellants designed to meet the required specifications are required not only to maintain their mechanical and ballistic integrity through sterilization cycles, but also to be free of any hazards associated with thermal explosions. The present study was undertaken (1) to assess the degree of hazard associated with the use of a series of candidate solid Jet Propulsion Laboratories (JPL) propellant formulations, (2) to investigate the application of small-scale laboratory experiments, limited larger-scale field tests, and known scaling laws to predict the onset of thermal explosions, (3) to investigate those aspects of ammonium perchlorate propellant decomposition which lead to thermal explosions, and (4) to observe the mechanical-physical change on heat cycling of solid JPL propellant grains.

THERMAL EXPLOSION STUDIES

ANALYSIS OF THERMAL EXPLOSIONS

In the sterilization of a rocket motor, it is desired to bring the body of the propellant to some high temperature and to maintain it at this temperature for a specified period of time. The temperature and time cycle must be selected in such a manner that the motor will be reasonably free of viable organisms. It is also necessary to assure that the temperature is not so high or the time so long that the motor will deflagrate spontaneously. For this reason, it is necessary to consider the factors which govern the onset of thermal explosions and evaluate the thermophysical and chemical properties of the propellants which are important in thermal explosion theory. With such information in hand it will be possible to design sterilization cycles for propellants which are free from thermal explosion hazards.

The phenomenon being considered involves the self-heating of propellant grains. Energy is liberated in the interior of the propellant grain due to slow chemical decomposition. If this energy is not liberated from the grain the temperature of the propellant will rise, increasing the reaction rate further. A balance point is reached at which the heat generated is equal to the heat liberated. This balance point is described by a critical temperature (T_m) for a given propellant in a particular geometry. When the decomposition kinetics are presumed to be

1

governed by zero-order kinetics the condition of a heated propellant will be described by the differential equation

$$-\lambda \nabla^2 T + \rho c \left(\frac{\partial T}{\partial t}\right) = \rho Q A e^{-E/RT} \tag{1}$$

Properties of this equation and its solution under a variety of conditions have been described before (Ref. 1, 2, 3, 4, 5). The decomposition of a small amount of propellant can generate a large amount of heat. Consequently, the amount of propellant decomposed just prior to thermal deflagration can be quite small. For this reason the zero-order model is quite appropriately applied to a number of explosion situations.

In the sterilization of a rocket motor the sample is heated to some reasonably high temperature for a fairly prolonged period of time. Under these conditions it is appropriate to examine the properties of Eq. 1 under steady-state conditions of $(\partial T/\partial t) = 0$. When the resulting equation is solved and rearranged it is found that there is a temperature T_m, (maximum surface temperature) which will permit the maintenance of a steady-state temperature within the body of the solid. If the surface temperature T_1 is such that $T_1 > T_m$ an explosion will result. If $T_1 < T_m$ then there will be no thermal explosion according to this zero-order model. T_m is given by:

$$T_m = \frac{E}{2.303R \log \left(\dfrac{\rho a^2 Q A E}{\lambda R T_m^2 \delta}\right)} \tag{2}$$

The values of the parameter δ for the slab, the solid cylinder, and the solid sphere are 0.88, 2.00, and 3.32 respectively. Some values of δ for hollow cylinders are given in Table 1 (Ref. 2). This critical temperature T_m is a key parameter used by Zinn and Mader (Ref. 4) and Zinn and Rogers (Ref. 5) and others to describe and predict thermal explosion properties. It was found (Ref. 4) and (Ref. 5) according to the model of Eq. 1 with the condition that the surface temperature $T_1 > T_m$ then the explosion time, t_e, is given by

$$\frac{t_e}{\tau} = F\left(\frac{E}{T_m} - \frac{E}{T_1}\right) \tag{3}$$

where the dimensionless time t_e/τ is a function of $(E/T_m - E/T_1)$.

2

TABLE 1. Shape Factors for the Hollow Cylinder.

Radius ratio	Shape factor, δ	
	Same temperature inside and outside	Adiabatic inside, constant temperature outside
0.025	3.008	2.003
0.05	3.320	2.020
0.10	3.892	2.077
0.15	4.492	2.172
0.20	5.171	2.306
0.25	5.966	2.483
0.30	6.921	2.713
0.35	8.091	3.004
0.40	9.556	3.384
0.45	11.43	3.878
0.50	13.88	4.530
0.55	17.19	5.413
0.60	21.81	6.646
0.65	28.55	8.434
0.70	38.91	11.17
0.75	56.10	15.69
0.80	87.73	23.92
0.85	156.1	41.57
0.90	351.3	91.50
0.95	1405	358.4
1.00	∞	∞

Here τ is the thermal time constant of the sample.

$$\tau = \frac{a^2}{\alpha} = \frac{\rho c a^2}{\lambda} \quad \text{where } (\alpha = \frac{\lambda}{\rho c}) \tag{4}$$

In the case of a solid cylinder, it was found (Ref. 4) that $(E/T_m - E/T_1) = 1.6$ when $t_e/\tau = 1$.
Thus, when $t_e = \tau$

$$\frac{1}{T_m} = \frac{1.6}{E} + \frac{1}{T_1} \quad \text{(E in cal/mole)} \tag{5}$$

A similar expression for the sphere is

$$\frac{1}{T_m} = \frac{0.65}{E} + \frac{1}{T_1} \quad \text{(E in cal/mole)} \tag{6}$$

When $t_e \neq \tau$, Fig. 3 of Ref. 4 gives the appropriate value of X in the equation:

$$\frac{1}{T_m} = \frac{X}{E} + \frac{1}{T_1} \tag{7}$$

Equations 3 through 7 permit the calculation of T_m for a given explosive material from one or from a series of measurements of t_e (explosion time) as a function of T_1 (ambient or surface temperature), provided a value of E is known. Once E and T_m are known, values of t_e for any imposed value of T_1 can be computed. These considerations apply as long as the zero-order model is effective and the amount of reactant consumed prior to deflagration is negligible.

At low temperatures near or even below T_m, the deflagration time (t_e) can be much longer than the thermal time constant (τ). Under these conditions it becomes necessary to apply a first-order model since reactant depletion effects become significant. Under these conditions the right hand side of Eq. 1 becomes $\rho \, QAwe^{-E/RT}$ and it is necessary to consider

$$dw/dt = -\alpha w e^{-E/RT} \tag{8}$$

Where w is the mass fraction unreacted at time, t.

4

However, when $t_e \gg \tau$ the propellant sample may be regarded as approximately isothermal and Eq. 8 may be integrated (Ref. 5) to give

$$t_e = - \frac{\ln(1-f)}{Ae^{-E/RT}} \tag{9}$$

where f is the fraction reacted at the time of deflagration. Since $Ae^{-E/RT}$ is the specific rate constant k

$$k = - \frac{\ln(1-f)}{t_e} \tag{10}$$

This equation permits the calculation of the specific reaction rate constant from deflagration time data if f is known. The value for f can be estimated from the k determined via DTA data.

The value of k can be calculated from deflagration data in two ways, depending on the test conditions. If the test is conducted at a temperature near or at the critical temperature of the test sample, the data under steady-state conditions with constant T (Eq. 1) can be integrated and as an approximation yields:

$$k = \frac{4\lambda}{Q\rho a^2} \left(T_c - T_1 \right) \tag{11}$$

where T_c is the center temperature (Ref. 1). The second technique involves an adiabatic condition where Eq. 1 is described for a no-heat transfer condition from the center of the propellant to some other point in the grain. This condition is given by Eq. 12

$$k = \frac{c}{Q} \left(\frac{dT}{dt} \right) \tag{12}$$

which measures the rate of temperature change with time at the geometric center of the sample. Under these conditions f can be calculated from Eq. 10 and with either Eq. 8, 11 or 12.

The temperature region of interest in sterilization studies is the region below T_m. This is the region where the zero-order theory predicts no deflagration, and deflagrations occur only as a result of first-order reaction effects when a significant quantity of the material has reacted.

5

The deflagration studies are carried out in the temperature range above T_m in order to provide a continuity for the study of effects in the low temperature, $t_e \gg \tau$, isothermal range.

EXPERIMENTAL TECHNIQUES FOR ISOTHERMAL ANALYSIS OF DEFLAGRATION TIMES

The propellants used in this study were of the PBAA - MAPO - AP type. Forty-eight solid and tubular, right-circular cylindrical propellant grains of various sizes and two 60-pound motors were prepared by JPL. All the propellant grains used for the deflagration and heat sterilization studies were of propellant batch no. JS-7 identified as HSP-X6 made with batch 5134 oxidizer and an equivalence ratio, PBAA to MAPO, of 1.5:1. The size, shape, and number of cylindrical grains used is shown in Table 2.

TABLE 2. Number and Dimensions of Samples (JS-7)

Charge shape	Charge size (OD x length, inches)			
	1 x 2.5	3 x 7.5	5 x 12.5	10 x 25
Solid cylinder	5	5	5	1
Tubular (d/D = 0.333)	5	5	5	1
Tubular (d/D = 0.500)	5	5	5	1

In isothermal analysis as customarily performed at the Naval Weapons Center (NWC), China Lake, Calif., propellant samples ranging in diameter from 0.1 to 12 inches with an L/D of one or greater can be processed. Since the sample size varies considerably, the type of oven used also varies.

For small samples (< 0.25 inch diameter) a quartz test tube (0.3 inch ID) in a tube-type furnace (Serial 634304, Marshall Products Co., Columbus, Ohio) is used. For all other samples up to 6 inches in diameter, standard cook-off ovens (8.5 inch ID) are used. These are made from 3/8-inch thick steel pipe, 8.5 inches in diameter, and 4 feet long. The pipe is covered with heating elements and is insulated within a transite box, 19 inches wide, 25.5 inches high, and 51.5 inches long. Lightweight fiberglass plugs approximately 6 inches long are used in each end of the oven. They are a tight fit to minimize convection heat losses, but release readily for the hot gases formed during deflagration. Samples above 6 inches in diameter are contained within a scaled-up standard cook-off oven.

6

Another kind of oven can be used in these studies. This oven is made of thick-walled aluminum tubing (from 0.5 to 1 inch thick) with dimensions to fit the sample being tested. A ribbon-type heater, about 1,000 watts, is wrapped on the outside of the tube.

For a test, the oven is preheated to a selected temperature before placing the sample in the oven. However, it is not practical to preheat an aluminum tube-type oven before introducing the sample. With larger test samples (>1 inch diameter), the sample is instrumented with thermo-couples (cross-sectional area at the center of the grain length) and wrapped in aluminum foil and then located centrally in the oven. The temperature of the oven is controlled with a time-proportioning action power supply. The power supply for the scaled-up (12 inch diameter samples) cook-off oven is of the on-off type with a variable range of about ±1°C.

The test is monitored remotely with a 6- to 24-point temperature recorder until deflagration occurs, or until the test is terminated. The data from this study are plotted as log time versus the reciprocal absolute temperature. The data from the instrumented samples on each test show the rate of temperature rise in the sample, and the occurrence of exotherms before deflagration or before the termination of the test. After a series of tests are completed at different oven temperatures, a plot of log time to the exotherm or deflagration versus the reciprocal absolute oven temperature is made. This type of plot shows a relation-ship between the tests performed until a point in temperature is reached where the line curves to approach some critical point in temperature below which deflagrations or exotherms would approach an isothermal condition. Generally, a test is designed for a deflagration or an exo-therm to take place within about 2 weeks.

RESULTS OF DEFLAGRATION TIME MEASUREMENTS

Most of the grains listed in Table 2 and one of the 60-pound motors were subjected to an evaluation of deflagration time as a function of temperature. Plots of the deflagration data on eight grains are shown in Fig. 1 through 10. All the data are summarized in Table 3. The time required for the surface of the grain to reach oven temperature was measured for each grain studied. This warm-up time was subtracted from the total elapsed time-to-deflagration. This gave a time-at-temperature or deflagration-time which was used in subsequent evaluations of the data. For comparison purposes, four grains were tested in the aluminum tube ovens described above. The warm-up time is very short in this type of oven.

All deflagration-time data (minus the warm-up time) was plotted as deflagration time versus 1/°K for the grains tested. The graphic display of this reduced data for the 1-inch diameters is given in Fig. 11, 3-inch diameters in Fig. 12, 5-inch diameters in Fig. 13, and 10-inch diameters

TABLE 3. Cook-Off Data for Various Propellants
With an L/D Ratio of 2.5.

Designation JPL BD -	Diam., in.	Grain type[a]	Oven type	Oven temp., °C	Total time to cook-off, hr	Time to cook-off at temp., hr
79/2	1	Solid	Air	193.3	11.6	9.6
78/3	1	Solid	Air	198.9	7.0	5.2
78/2	1	Solid	Air	201.7	6.5	4.3
79/3	1	Solid	Air	219.4	2.9	1.2 - 0.1*
79/7	1	Tub.-1/3	Air	215.6	3.0	1.2 - 0.2*
79/6	1	Tub.-1/3	Air	226.7	1.7	0.65 - 0.2*
78/5	1	Tub.-1/2	Al	207.2	NCO[b]	---
79/4	1	Tub.-1/2	Air	218.9	2.0	0.9 - 0.2*
79/5	1	Tub.-1/2	Air	223.9	1.8	0.73 - 0.2*
71/5	3	Solid	Air	160.0	NCO[c]	---
81/2	3	Solid	Al	165.6	NCO[d]	---
77/2	3	Solid	Air	166.1	62.5	53.0
76/2	3	Solid	Air	177.8	35.7	24.7
80/4	3	Solid	Al	172.2	33.6	33.6
77/4	3	Tub.-1/3	Air	183.3	23.0	17.0
76/4	3	Tub.-1/3	Air	183.3	22.0	17.0
81/4	3	Tub.-1/3	Al	187.8	16.5	16.5
71/6	3	Tub.-1/3	Air	190.6	11.5	7.0
81/3	3	Tub.-1/2	Air	190.6	11.8	6.3
80/3	3	Tub.-1/2	Air	196.7	9.8	3.8
76/3	3	Tub.-1/2	Air	201.7	8.0	2.5
68/3	5	Solid	Air	164.4	84.9	70.9
83/2	5	Solid	Air	165.6	58.7	43.2
69/6	5	Solid	Air	177.2	35.2	18.7
70/6	5	Solid	Air	176.7	40.5	23.5
82/2	5	Solid	Air	182.8	32.0	12.0
69/4	5	Tub.-1/3	Air	167.2	63.3	52.3
68/2	5	Tub.-1/3	Air	176.7	34.8	22.8

TABLE 3. (Continued)

Designation JPL BD -	Diam., in.	Grain type[a]	Oven type	Oven temp., °C	Total time to cook-off, hr	Time to cook-off at temp., hr
82/4	5	Tub.-1/3	Air	182.8	24.6	14.1
68/6	5	Tub.-1/2	Air	173.9	32.8	20.3
82/3	5	Tub.-1/2	Air	182.2	28.0	16.0
8 1/4	5	Tub.-1/2	Air	191.1	7.3	2.8
71/2	10	Solid	Air	153.3	---[e]	---
77/6	10	Tub.-1/3	Air	156.7	151.5	106.5
78/9	10	Tub.-1/2	Air	156.7	129.5	94.5
79/9	10	Tub.-1/3	Air	162.8	74.4	---
82/6	10	Tub.-1/3	Air	168.9	67.7	37.7
87/1	10	Tub.-1/2	Air	168.9	86.7	36.7
Motor[f]	12	Tub.-1/2	Air	163.3	86.4	72.4

[a] Tub. = Tubular grain, ratio = inside diameter/outside diameter.

[b] No cook-off. A 5.6°C exotherm after 2.4 hours and a 14.4°C exotherm after 5.1 hours.

[c] No cook-off to 116.7 hours, oven temperature then increased 16.7°C, cook-off occurred at 5 hours.

[d] No cook-off to 167.4 hours. Cook-off in 70.4 hours at 176.7°C. (Temperature raised to 176.7°C after 167.4 hours.)

[e] Cook-off at 77.5 hours on second cycle.

[f] L/D ratio = 1.

[*] Time in hours allowed for AP crystal transition to take place.

in Fig. 14. The experimental critical temperatures (Table 4) were determined from the above plots on each size via Eq. 4 and 5 using the indicated $1/T_1$ values shown on Fig. 11 through 14. The experimental critical temperature corresponds to a sudden change in the above plots of deflagration time versus temperature. In the plot of 10-inch diameter grains, there was not a sufficient number of grains available for testing to show this effect. Since only ne deflagration test was made using a grain cast in motor hardware, a reduced time plot (i.e., Fig. 11 through 14) could not be accomplished. The critical temperature determined from this single test and Eq. 4 and 5 was 155°C.

TABLE 4. Critical Temperature Data on
JS-7 Propellant (δ = 2.00).

Diameter of Grain (inch)	T_m, °C[a]	T_m, °C[b]
1	212.2	215.0
3	181.7	186.7
5	168.9	173.9
10	152.2	157.2
12	148.3	155.0
30	128.9	(136.7)*

[a] Based on DTA kinetic data.

[b] Based on deflagration data.

* Based on experimental data from Fig. 15.

A plot of these values for the experimental critical temperature versus diameter is given in Fig. 15. Also included is a plot of the DTA predicted critical temperature. The experimental and predicted critical temperature values are close, but the experimental critical temperature value indicates a slightly higher activation energy (34.2 kcal per mole) than that predicted by DTA (33.3 kcal per mole). The values for T_m obtained from these experiments are compared with those obtained from DTA studies in Table 4. The data indicate that the first DTA exotherm controls the deflagration. The reduced data plots for each size show several different conditions concerning these grains. One is that these deflagration tests show an isothermal condition cannot exist in a tubular grain without having a large heat sink available to maintain a constant surface temperature. The aluminum foil used inside the tubular grains was not sufficient to maintain constant surface temperature and the inside surface of these grains approached an adiabatic condition. In such a condition, the shape factor does not change greatly from that of a solid. A shape factor of 2.0 was used in all of these calculations.

The other feature is that at relatively low temperatures, where $T_1 < T_m$ such that deflagration times are much longer than the reduced time (Eq. 4), the chemical reaction or decomposition can be regarded as approximately isothermal and the deflagration times could be determined by Eq. 9 and 10. At a temperature where $T_1 > T_m$, the isothermal approximation would not apply and the deflagration times would be shorter.

Data from grains that deflagrated at temperatures below their critical temperature were used to calculate the fraction reacted, f, at the time of deflagration. This was accomplished by using Eq. 9, 10, and 11. The value obtained for f was 0.073. The data calculations are given in Table 5.

10

TABLE 5. Extent of Reaction, f, Calculations at
the Time of Deflagration.

Test no. BD -	Grain size, in.	t_e/a^2, sec/cm^2	$T_c - T_1$, °C	f^a	Oven type
68/3	5	6.33 x 10^3	1.94	0.107	Air
83/2	5	3.86 x 10^3	1.66	0.057	Air
70/6	5	2.1 x 10^3	2.22	0.042	Air
69/6	5	1.67 x 10^3	2.22	0.034	Air
80/4	3	8.24 x 10^3	1.66	0.12	Al
77/2	3	13.1 x 10^3	0.55	0.065	Air
76/2	3	6.12 x 10^3	1.66	0.089	Air

[a]Average value of f = 0.073.

Since Eq. 9 is independent of mass, a plot of time to deflagration after attaining test temperature versus this test temperature was determined for all grain sizes tested below their critical temperature. The plot is shown in Fig. 16. The slope of this plot has a value of 26.2 kcal per mole for the activation energy.

THERMOANALYTICAL STUDIES

ANALYSIS OF THERMOANALYTICAL DATA

The ability of a propellant to survive the sterilization environment is dependent in large measure on the kinetics of its thermal decomposition reactions. If appropriate rate parameters were known they could be used together with the equations described above to make a proper assessment of the susceptibility of a given propellant grain to thermal explosion.

Two small-scale laboratory techniques, differential thermal analysis (DTA) and thermogravimetric analysis (TGA) have been employed in this study to measure the decomposition parameters of JPL propellants. These are particularly appropriate since they measure quantities (heat evolution and weight loss) which are particularly related to thermal explosions, and because they are conveniently and rapidly applicable to solid propellants. As such, these techniques would be most valuable for the purpose of screening candidate propellant formulations if their relationship with thermal explosion behavior could be established.

11

Differential thermal analysis involves continuous measurement of the temperature difference between a small sample (usually 10 to 75 mg) and a thermally inert reference material, as a function of the sample or reference temperature and/or time, as both the sample and reference material are heated simultaneously at a predetermined rate. When a reaction occurs, changes in the heat content and in the thermal properties of the sample are indicated by a deflection or peak which shows on the graphic record. If the reaction proceeds at a rate varying with temperature (i.e., possesses an activation energy), the position of the peak varies with the heating rate, providing that other experimental conditions are maintained fixed (Ref. 6 and 7). Five or more DTA runs are made at different selected constant heating rates for each sample.

The decomposition rates associated with the exotherms are determined in the following manner. The activation energy and frequency factor are determined by the modified variable heating rate method (Ref. 2 and 8) in which is plotted, for a particular exotherm, the log-heating rate over the absolute peak temperature squared versus the reciprocal absolute peak temperature. The absolute peak temperature is taken with respect to the reference temperature rather than the sample temperature. In the thermal stability studies, the exotherms occurring in the lower temperature ranges of a thermal pattern are evaluated first. With this type of graph the activation energy (E) calculations are made, based on the equation (Ref. 6):

$$\frac{d \log (\phi/T_{rp}^2)}{d (1/T_{rp})} = - \frac{E}{2.303 \ R} \tag{13}$$

Once the above values for E are known, the frequency factor (A) $(\sec^{-1})$ can be calculated from Eq. 14, assuming the order of reaction to be unity.

$$\frac{E \ \phi}{R \ T_{rp}^2} = Ae^{-E/RT_{rp}} \tag{14}$$

The determination of the specific rate constant k $(\sec^{-1})$ can be made using the E and A values and the Arrhenius rate equation:

$$k = Ae^{-E/RT} = \frac{2.303}{t} \log \left(\frac{C_o}{C_1}\right) \tag{15}$$

12

Values for k can be determined at selected temperatures. The specific rate constant can be used in estimating the percent reacted for a given endothermic or exothermic peak. The temperature (T) is absolute, time (t) is in seconds, with C_0 the initial concentration, and C_1 the concentration after a specific time and at a specific temperature. The actual concentrations need not be known for calculations since first-order or pseudo first-order reactions are assumed.

A second method for obtaining kinetic data from a DTA thermal profile is the area method proposed by Borchardt and Daniels (Ref. 9) and Reed, et al (Ref. 10). The method is based upon Eq. 16, where the heat capacity of the sample is assumed to be quite small compared with the heat of reaction.

$$k = \frac{\Delta T}{|A_t|} \tag{16}$$

where ΔT is the temperature difference between the sample and reference material (deviation from the base-line) and is proportional to the rate of reaction at the sample temperature. The quantity $|A_t|$ is the difference between the area under the entire thermogram peak and the area trace-out up to the particular temperature T. The value of $|A_t|$ is assumed to be proportional to the amount of unreacted material. The activation energy and frequency factor are determined from Eq. 15. By using the area method, kinetic parameters can be determined from a single DTA pattern, providing the exotherms do not overlap.

Inherent in the development of both these methods of treating DTA results is the assumption that the rate of reaction is independent of time. The low temperature decomposition of ammonium perchlorate and of ammonium perchlorate propellants does appear to be time dependent and the application of the Kissinger method and the area method should be regarded as procedural kinetic rate measurements. Because of the existence of an "induction period," and because the "induction period" may vary with temperature, the kinetic results should be regarded as only approximate.

The TGA technique is also applicable to the study of propellant decomposition. Thermogravimetric analysis consists of the continuous, or frequently repeated measurement of the weight, or change-in-weight of a specimen as it is subjected to a temperature program. Generally, it will include automatic and continuous recording of weight, or change-in-weight, as the sample is subjected to a constant temperature, or to a selected uniform, or changing, dynamic heating rate. The temperature programming and/or control is usually of the same general nature as for differential thermal analysis and for isothermal analysis.

EXPERIMENTAL THERMOANALYTICAL TECHNIQUES

The differential thermal analysis apparatus used in these studies was designed and fabricated at NWC. This apparatus, which is operational to approximately 450°C, is described as follows:

The sample (usually 10 to 75 mg) is massed about the tip of the thermocouple probe which is housed within a glass reaction tube[1]. The reaction tubes are constructed of Pyrex, 3/8 inch diameter and approximately 5 inches long, with a 10/30 ground glass female joint on the upper end. A glass sidearm is attached to the midpoint of the reaction tube. The sidearm extends at a 45 degree angle for about 2.25 inches, then horizontally for about 3 inches. This sidearm can be employed advantageously in a number of applications, e.g., (1) addition of glass beads without contamination of the ground glass joints, (2) for making runs under dynamic gas flow systems, (3) for containment of toxic reaction products by utilizing a balloon or by exhausting the products to an exhaust port via a flexible tube, (4) for maintaining the dry-box condition of the sample within the reaction tube by the use of a balloon or a drying tube, and (5) for drawing a partial vacuum on the sample.

The thermocouple probes, which have ground glass male joints, are placed within the reaction tubes; the ground glass joints give a secure, leak-free connection. The reaction tube is filled with glass beads (0.05 - 0.1 mm diameter) through the sidearm of the tube to completely cover the sample and probe tip. A second reaction tube, containing the inert reference probe, is filled only with the glass beads. A third reaction tube contains a thermocouple probe which is arranged in a manner similar to the inert reference tube, and the output from this thermocouple is used to record the actual reference temperature simultaneously with the differential thermal temperature from the sample and reference thermocouples. All three reaction tubes are filled with glass beads up to identical levels, approximately 0.5 inch. The three reaction tubes are inserted into their respective wells in the aluminum heating block (2.25-inch diameter x 3-inch long cylinder); the cylinder is placed within a pint-size Dewar flask, which affords protection against rapid heat loss and yields a more uniform heating rate.

The heating unit, a tube-type 140-watt cartridge heater, is located within the center of the aluminum block. It is connected to and controlled by a power proportioning temperature programmer (Model 240M-00, Hewlett-Packard Co., Palo Alto, California). The programmer senses the temperature of the block by means of a thermocouple located within the block, midway between the two sample wells. The differential output from the sample-inert reference thermocouples is transmitted to the microvolt amplifier (DC microvolt-ammeter, Model 425A; Hewlett-Packard Co., Palo Alto, California) and then fed into a two-pen potentiometric recorder which produces a thermal pattern (thermogram) as the temperature of the system is increased in a linearly controlled manner. However, the

---

[1] A schematic drawing of a similar-type tube with slightly varying dimensions is shown in NOTS TP 2748.

14

amplifier is not necessary if a properly equipped Honeywell Model 194 recorder is used. The recorder can be adjusted to give a zero reading at any portion of the chart, thus both endothermic and exothermic reactions can be recorded adequately. On the same chart, the temperature of the system is recorded simultaneously with the thermogram. This permits the direct determination of any temperature level on the DTA thermogram and, since the chart speed is known, the true heating rate can be determined easily. This type of DTA equipment, with minor modifications, has been in use for over 6 years and has produced several thousand thermal patterns.

For TGA studies, a Cahn elecrobalance is used to continuously weigh a sample (usually 50 to 100 mg) as a function of temperature and/or time. This balance (Ventron Instrument Corp., Cahn Division, 7500 Jefferson Street, Paramount, California) is a null-point instrument in which a light source photocell is the detector and an electromagnetic D'Arsonval movement supplies the restoring force. The loop gain of the servo system is in excess of 1,000, so that the actual beam deflection under load is very small, and the balancing torque is essentially equal to the sample torque. The torque motor used in the balance is as linear as precise weights and precision potentiometers can determine. Thus, the balancing current is a direct measure of the sample weight to an accuracy of better than ±0.1% and a precision of better than ±0.01% of full scale sample weight.

Any change in sample weight causes the balance beam to move. This motion is detected by the change in photocell voltage because of the movement of the shutter attached to the beam, which interrupts a light source. The photocell voltage is amplified and then applied to the coil attached to the beam. The coil is in a magnetic field and current passing through it exerts a force on the beam, restoring it to a null position. The coil current is thus a measure of sample weight.

RESULTS OF THERMOANALYTICAL STUDIES

Propellants JS-1, JS-2, JS-3, and JS-7 were studied in the DTA apparatus. The identification and the equivalence ratio, PBAA to MAPO, for the four propellant samples were HSP-X4 (1:3), HSP-X5 (1:1), HSP-X6 (1.5:1) and HSP-X6 (1.5:1), respectively. Cup type thermocouples were used for these materials in the representative thermograms shown in Fig. 17. Point-junction type thermocouples were used for obtaining the kinetic runs for the four propellants as shown in Fig. 18 through 29.

The results of the kinetic study are plotted in Fig. 30 through 33 respectively, for JS-1, JS-2, JS-3, and JS-7. The JS-1 gave very erratic results, even on a repeat DTA study. This may be due, in part, to the overlapping of the first and second exotherms. The activation energy as determined by Eq. 14 was about 15 kcal per mole. This is a very low value

15

for E and may be due to the high concentration of MAPO present in the propellant. The JS-2 propellant had an activation energy of 33.2 kcal per mole as determined by Eq. 14 for the first exothermic peak while the JS-3 propellant had a value of about 27 kcal per mole. The study on JS-2 and JS-3 propellants was limited to results from the DTA tests. The JS-7 propellant was studied more in detail than the other propellants since JPL had selected this propellant for the deflagration and heat sterilization test grains. For the JS-7 propellant, the activation energy for the first exotherm was 33.3 kcal per mole, using Eq. 14. The area method (Eq. 15 and 16) for this exotherm gave 31.4 kcal per mole, which used only the peak value of each DTA. The plot is shown in Fig. 34. The area method results are similar to the results obtained by using the variable heating rate method. The area method results are given for comparison purposes only and were not used in predicting the critical temperature.

In predicting the critical temperature from the DTA data using Eq. 2, certain values had to be obtained for the density, heat capacity, and thermal conductivity. The density, ρ, was given by JPL as 1.76 g/cm^3. The heat capacity, c, was estimated at 0.3 cal/g. The thermal conductivity, λ, was measured from 3- and 5-inch diameter solid grains of the propellant when they were being heated in an air-type oven. The equation used for determining the thermal diffusivity (α) is given as:

$$\alpha = \frac{a^2}{4\Delta T} \left(\frac{dT}{dt}\right) \qquad (17)$$

where:

$\frac{dT}{dt}$ = heating rate at the surface of the grain (°C/sec) and

$\lambda = c\rho\alpha$

The average value for λ was 0.00053 cal/(cm)(sec)(°K). The predicted temperature values for different sizes and shapes of JS-7 propellant are given in Table 4.

Weight-loss studies were also performed on small samples (~100 mg) of JS-7 in the temperature range of 193 to 232°C. The sample would initially lose about 0.7% of its weight at the selected test temperature. After this initial loss, the sample would lose weight slowly as would be expected, but after a time depending on the test temperature, the weight loss rate would increase very rapidly. This temperature dependency of the weight loss rate was plotted as an Arrhenius function using Eq. 15. This plot is shown in Fig. 35. The two weight loss steps in Fig. 35 show about the same activation energy of 34 to 35 kcal per mole but

16

differ in rate of decomposition by about a magnitude of 10. This would indicate that the decomposition paths are the same in each case, but that the faster or third weight-loss step is either dependent on the second weight-loss step or on some other time delay function. Both weight-loss steps appear to have about the same decomposition path as the first DTA exotherm also shown in Fig. 35.

EFFECT OF SIZE ON HEAT STERILIZABLE
SOLID PROPELLANT CHARGES

An experimental program was carried out to determine the number of 135°C heat cycles that would produce cracking or voids in propellant charges of various sizes and shapes. One cycle would consist of the time to heat the slowest-heating portion of the charge to 134°C (as measured by the thermocouple in the control sample) plus 53 hours at 135 ± 1°C. The heat cycle time would not include the cool-down period. Visual inspection and possibly photographic coverage would be made on each charge prior to and after each cycle.

The test (heat) cycle, for each diameter size, was determined by employing a charge that contained a thermocouple which was located within the geometrical center of the propellant mass. The ovens were of the same types used for the deflagration studies. The setup was monitored closely to determine the time lapse (dwell time) from the moment of sample insertion into a preheated oven to the time when the internally located thermocouple reached 134°C. The internal temperature of the charge was then maintained at 135 ± 1°C for 53 hours. It required 2 to 3 cycles to obtain the correct operational parameters. Subsequent cycles were then run at the same operational oven temperature for identical time periods. Usually, a second sample, same diameter but without an internal thermocouple, was run under the established operational parameters.

The 3-inch diameter propellant charge required 6 to 7 hours of dwell time in a preheated oven before the internally located thermocouple reached 134°C; the dwell times for the 5- and 10-inch diameter charges ranged from 29 to 30 and 45 to 53 hours, respectively. It was determined that the duration of the test cycles for the 3-, 5-, and 10-inch diameter charges would be 60, 82.5, and 104 hours, respectively; the duration included dwell time plus 53 hours at 135 ± 1°C. The test cycle was terminated by withdrawing the charge from the oven. This was accomplished by employing a sled-like device that held the charge and also pulled forth an oven closure-port when the charge was removed remotely at the completion of the cycle. After the charge was removed from the oven, it was allowed to approach the ambient air temperature. For the 3-inch diameter charges, the internal temperature was reduced quickly to 42-50°C after only 3 hours and to 37°C after an additional 2-hour period. However,

17

for the 10-inch diameter charges much longer cooling periods were required, as the larger mass afforded better insulation. The internal temperature of the 10-inch sample was reduced to 88-90°C after 10 hours and to only 63-66°C after an additional 6 hours. Observations were made on the samples at the completion of each test cycle. In addition, X-ray pictures were taken of the 12-inch motor after the first and second cycles, and they were sent to the Jet Propulsion Laboratory. The results of the cycling tests on the 3-, 5- and 10-inch diameter samples are summarized and depicted graphically in Fig. 36.

Because of the mass effect, it requires more time for the center of a larger solid grain than for the center of a smaller grain to reach 134°C when both are placed simultaneously within a preheated 134 to 135°C oven. Therefore, the durations of the test (heat) cycles, used in preparing Fig. 36, were adjusted to compensate for this difference. First, the temperature-time data obtained from a thermocouple located within the geometrical center of the charge was plotted (Fig. 37 through 39). Then, a tangent was drawn for each curve, as illustrated. The intercept of the tangent with the sterilization temperature level gave the time correction value for each diameter. The test (heat) cycle periods of 60, 82.5, and 104 hours were adjusted to give 54, 69, and 75 hours for the 3-, 5-, and 10-inch-diameter charges, respectively. The adjusted values were utilized in preparing the data presented in Fig. 40. This plot shows the apparent empirical relationship between the diameter and the time to the appearance of cracks or voids when the propellant charges are held at the sterilization temperature level. Figure 40 also shows the period (not adjusted) when cracks were observed first.

A 60-pound, 12-inch diameter motor, with a d/D ratio of 1/3 and a L/D ratio of 1, and containing JS-7 propellant, was cycled until the motor failed. The propellant thermocouples (Fig. 41) were inserted at the nozzle end and then fed out through the igniter opening. Before the start of the first cycl , both the igniter and the nozzle ends were sealed and then pressure tested at about 20 psia for leaks. The period of cycling for the motor was monitored by thermocouple No. 2 located at the inside surface of the propellant grain (Fig. 41). During the first test cycle, the oven temperature had to be raised carefully to avoid "over-shooting" the target temperature of 135 ± 1°C inside the motor. On the second cycle test, the oven temperature had to be increased by 1°C so that the lower limit would be reached. Apparently, some self-heating occurred during the first test cycle. The initial oven controller temperature was set at 138°C, then during the second test cycle the oven controller setting was raised to 143°C, and this setting was maintained for the remaining tests. The controller temperature oscillations ranged between 0.6 to 0.8°C. The third and fourth cycles were the same in regards to the overall length of time and temperature. During the latter two cycles, the motor required a dwell time of 36 hours within the preheated oven before the inside surface of the propellant grain acquired a temperature of 134°C.

18

At the completion of each test cycle the motor was removed from the oven and was allowed to cool to the ambient air temperature. The temperature at the inside surface of the propellant grain was reduced to 93°C after 5 hours, to 66°C after 8 hours, and to 38°C after a total of 20 hours.

The propellant in the motor was cracked badly after the first test cycle (Fig. 42 and 43). An attempt was made to determine when the propellant first started to crack, from an examination of the temperature record, but this could not be done. The condition of the propellant remained about the same throughout the second and third cycles (Fig. 44). After completion of the fourth cycle, it was observed that the propellant in the motor had bulged and swelled (Fig. 45). The outside motor case did not appear to have been affected by the bulging propellant. This motor was returned to JPL.

In a deflagration study done previously on a 12-inch diameter motor with a similar propellant type, it was determined that this motor had a critical temperature of about 155°C. This would mean that at about 155°C or higher, self-heating would have an effect on the time to deflagration. Below 155°C, the self-heating effect would diminish and the time to deflagration would follow a first-order decomposition path under isothermal conditions. In the sterilization temperature region, some degradation effects were apparent in the instrumented 12-inch motor when it was observed that bulging and swelling occurred during the fourth sterilization cycle.

The thermal stability of an ammonium perchlorate propellant is very important in this study as the propellant must maintain its mechanical and ballistic integrity after being subjected to the rigorous sterilization cycling procedure. A detailed kinetic study was not performed on the ammonium perchlorate itself as it has been studied and reported by numerous investigators. However, inhouse quality control studies have indicated that the purity of the oxidizer is a determining factor when thermal stability characteristics are evaluated. Even though high purity ammonium perchlorate could be used, the PBAA binder might still catalyze the low temperature decomposition of the ammonium perchlorate. Therefore, the binder should be as inert as possible in this temperature region of sterilization. This is brought out when the different types of propellants used in other studies were examined. It was possible to show the effect of various ingredients on the critical temperature as shown in Fig. 46. In this figure, the data for the prediction of the critical temperature were taken from DTA and isothermal analysis studies. The reference line at the 3-inch diameter grain was picked arbitrarily since most deflagration studies were conducted with 2- to 5-inch diameter samples. The dividing lines shown between different propellant ingredients are only approximate temperature limits and they are based on information found with the propellants listed. For comparison, the data on the JS-7 propellant is included. The figure shows that to gain more stability,

19

the long chain polymers and fluorocarbons are likely candidates for binder material. For the oxidizer, high purity ammonium perchlorate, specially stabilized ammonium perchlorate, or potassium perchlorate would be necessary.

CONCLUSIONS

This study has shown that kinetic data from DTA and isothermal analysis studies can be used to predict the thermal stability of propellants. These techniques can also be used to predict the thermal stability of explosives, pyrotechnics, and other materials that exhibit exothermic reactions, provided the kinetic parameters can be determined by thermal analysis. The results of a prediction can be given in precise terminology, e.g., terms that relate geometry (mass), time, and temperature. This will eliminate the possibility of performing tests under any set of conditions, tending to yield almost any type of data desired. It is possible, however, to relate and correlate results from data obtained by different persons with different types of instrumentation.

Of the four propellants studied with the polybutadiene type binder, the JS-7 propellant appears to be the most thermally stable. The kinetic studies have shown a difference in the thermal stabilities of four propellants that were very similar in composition. This shows that small changes in formulations can directly affect the thermal stability and indirectly affect the aging characteristics of propellants.

A 60-pound 12-inch diameter JS-7 propellant grain, cast in motor hardware, underwent four sterilization temperature test cycles. Although the propellant cracked badly during the first cycle, it was not until the fourth cycle was completed that it was possible to observe any noticeable bulging and swelling of the propellant grain. The outside motor case did not appear to have been affected by the bulging propellant. The cracking of the propellant was a physical type action (possible post-curing) while the bulging was the result of chemical decomposition reactions.

20
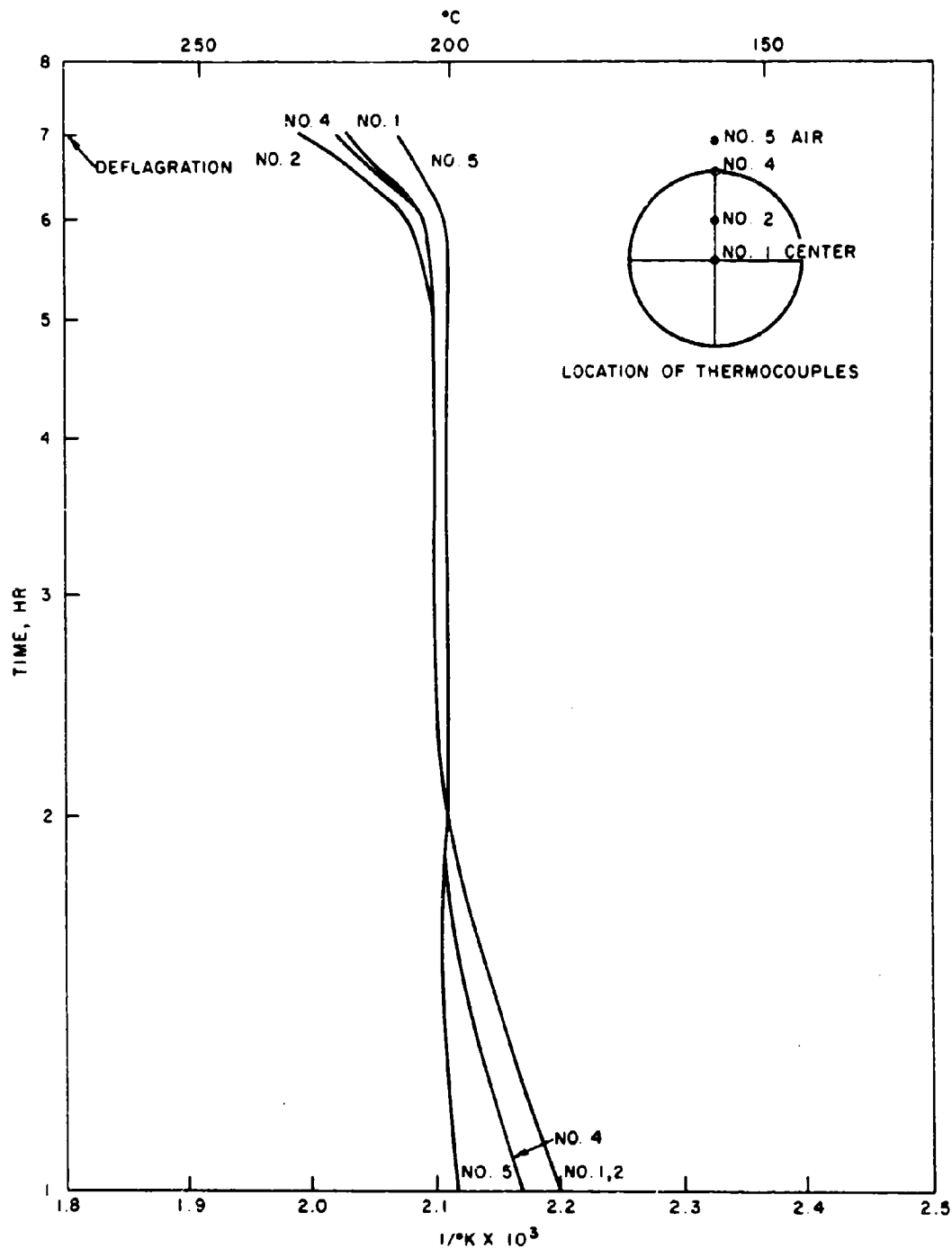
FIG. 1. Thermal Profile for a 1-Inch Diameter x 2.5-Inch Long Solid
Cylinder of JPL Propellant (BD 78/3) in a 198.9°C Oven.
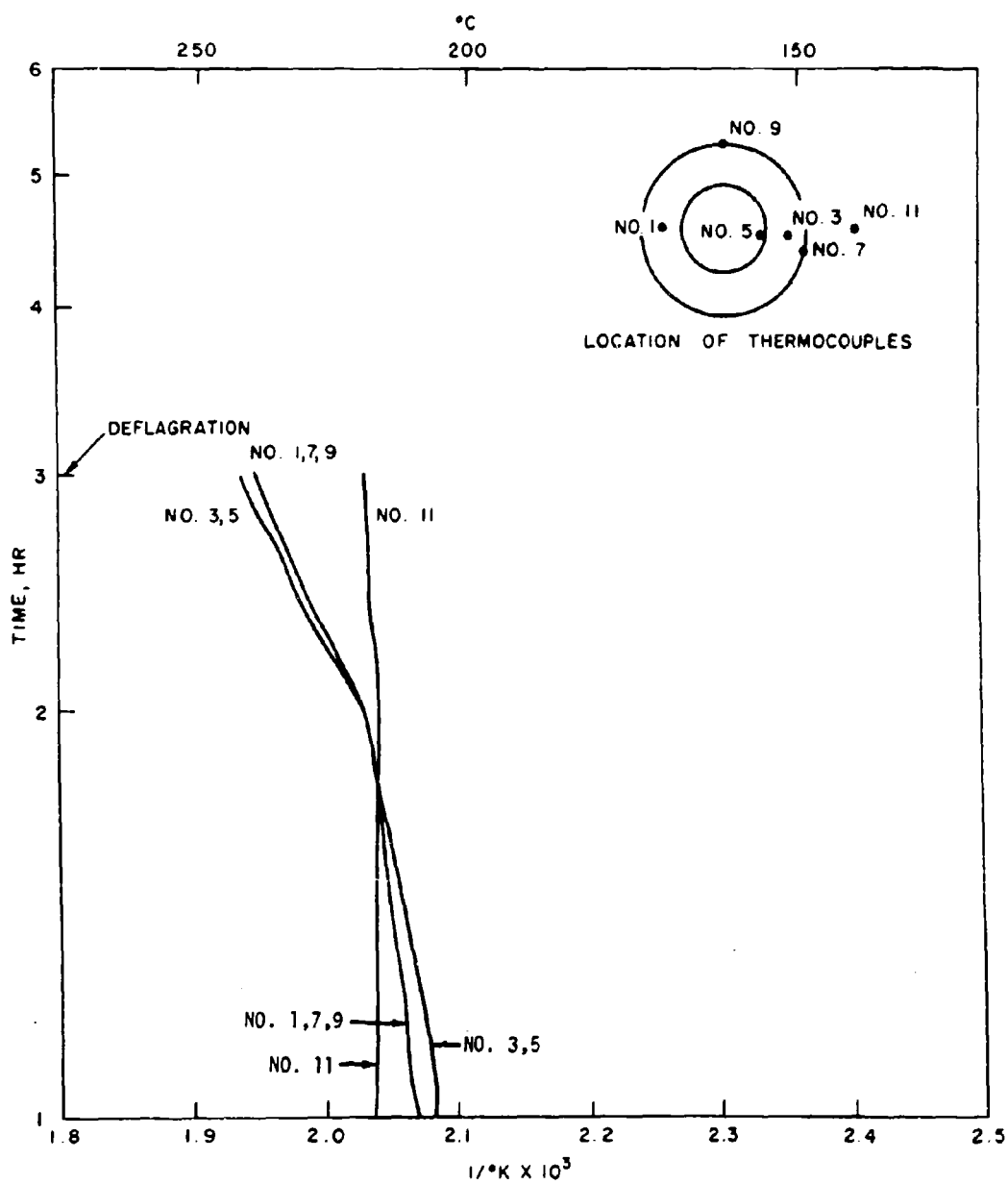
FIG. 2. Thermal Profile for a 1-Inch Diameter x 2.5-Inch Long Tubular Cylinder of JPL Propellant (BD 79/7) in a 215.6°C Oven.

22
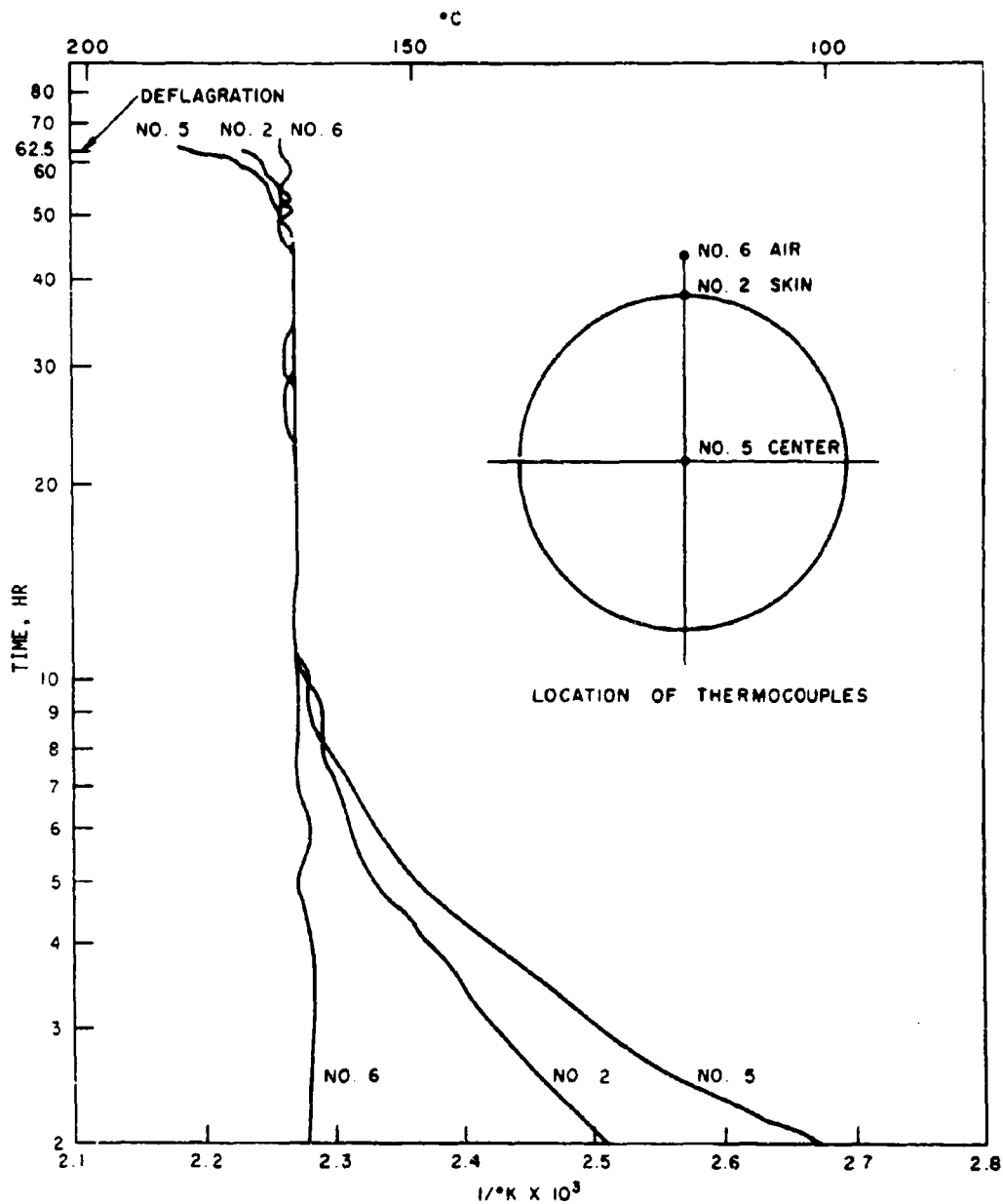
FIG. 3. Thermal Profile for a 3-Inch Diameter x 7.5-Inch Long
Solid Cylinder of JPL Propellant (BD 77/2) in a 166.1°C
Oven.

23
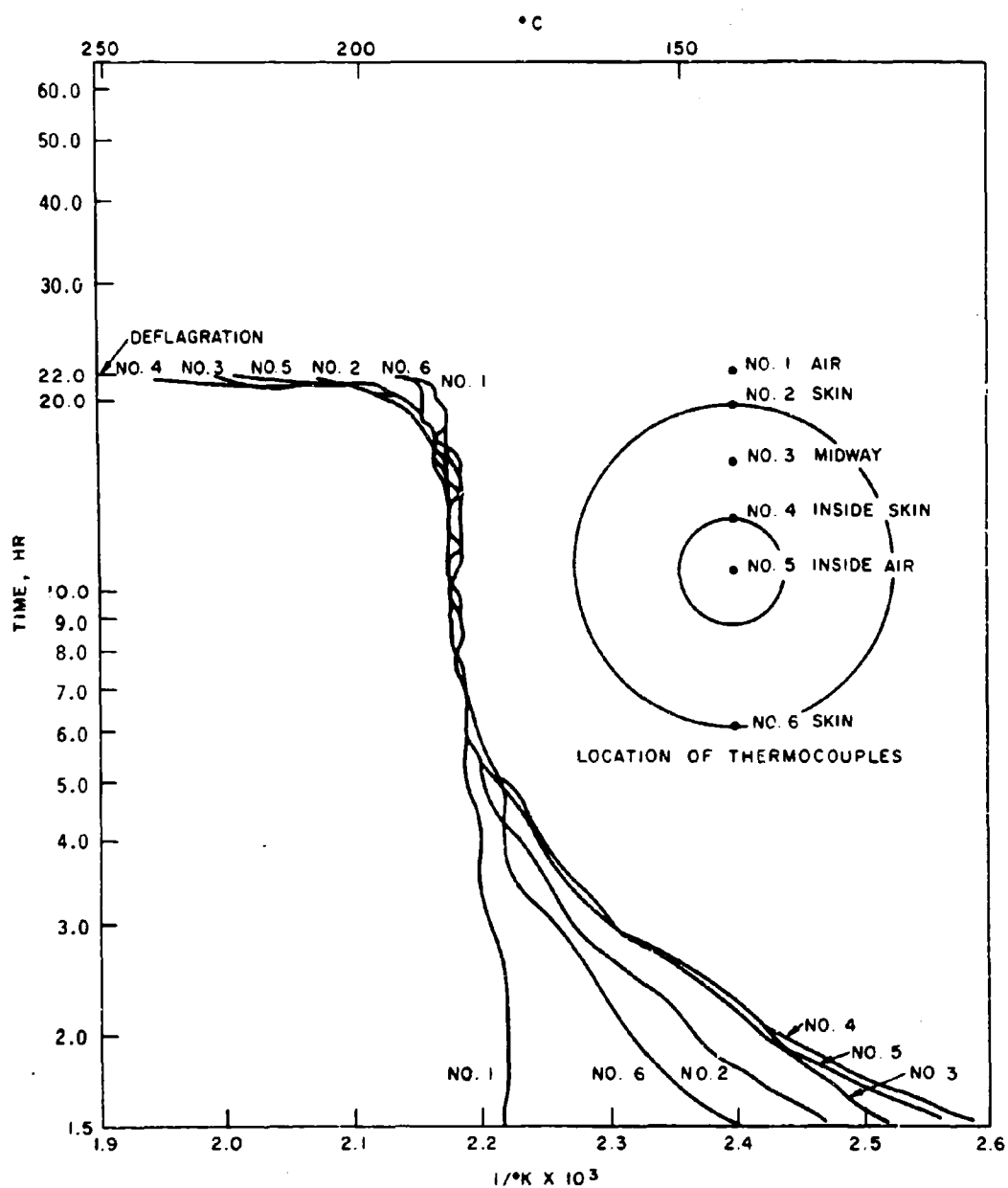
FIG. 4.   Thermal Profile for a 3-Inch Diameter x 7.5-Inch Long
Tubular Cylinder of JPL Propellant (BD 76/4) in a
183.3°C Oven.
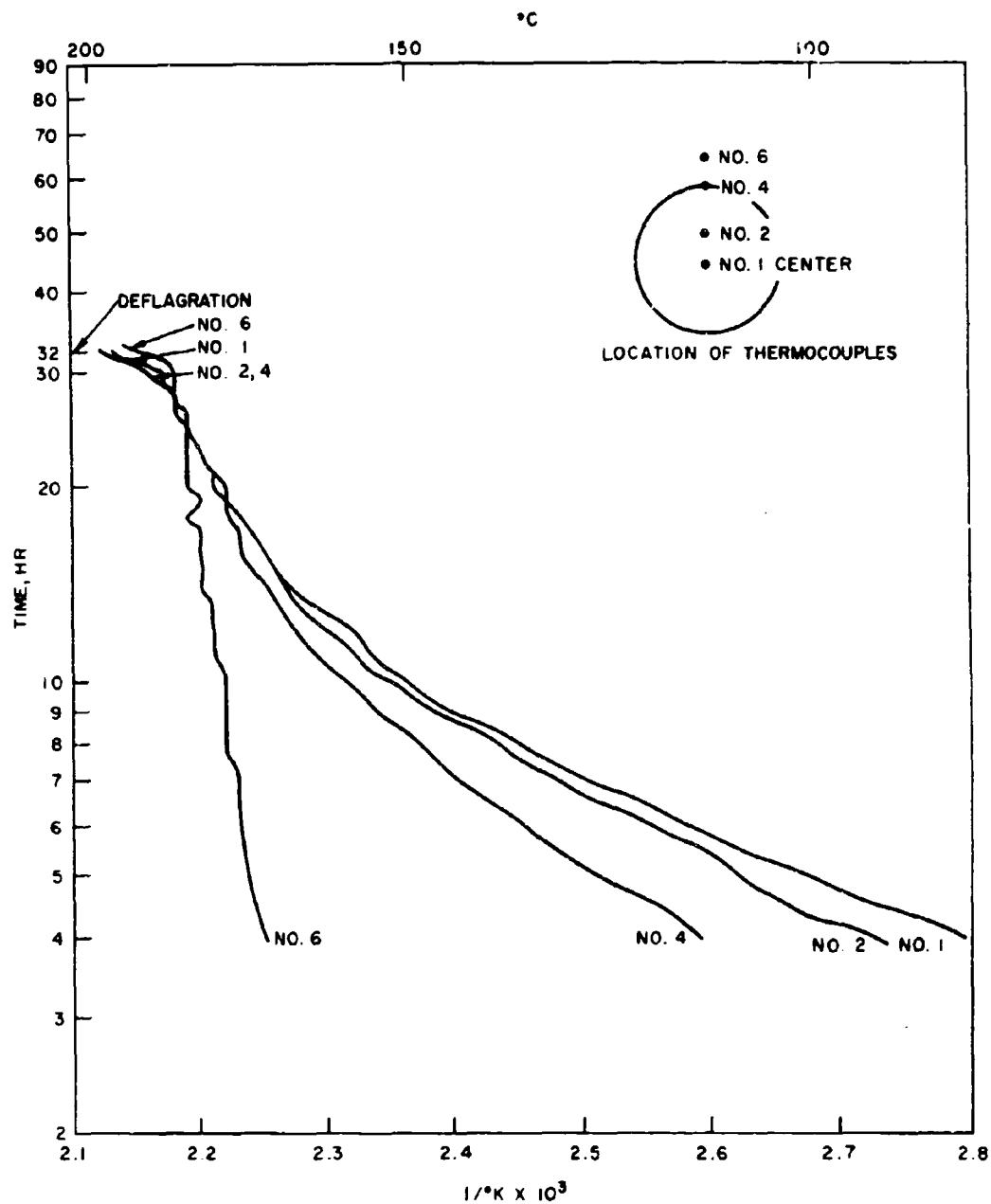
FIG. 5. Thermal Profile for a 5-Inch Diameter x 12.5-Inch
Long Solid Cylinder of JPL Propellant (BD 82/2)
in a 182.8°C Oven.
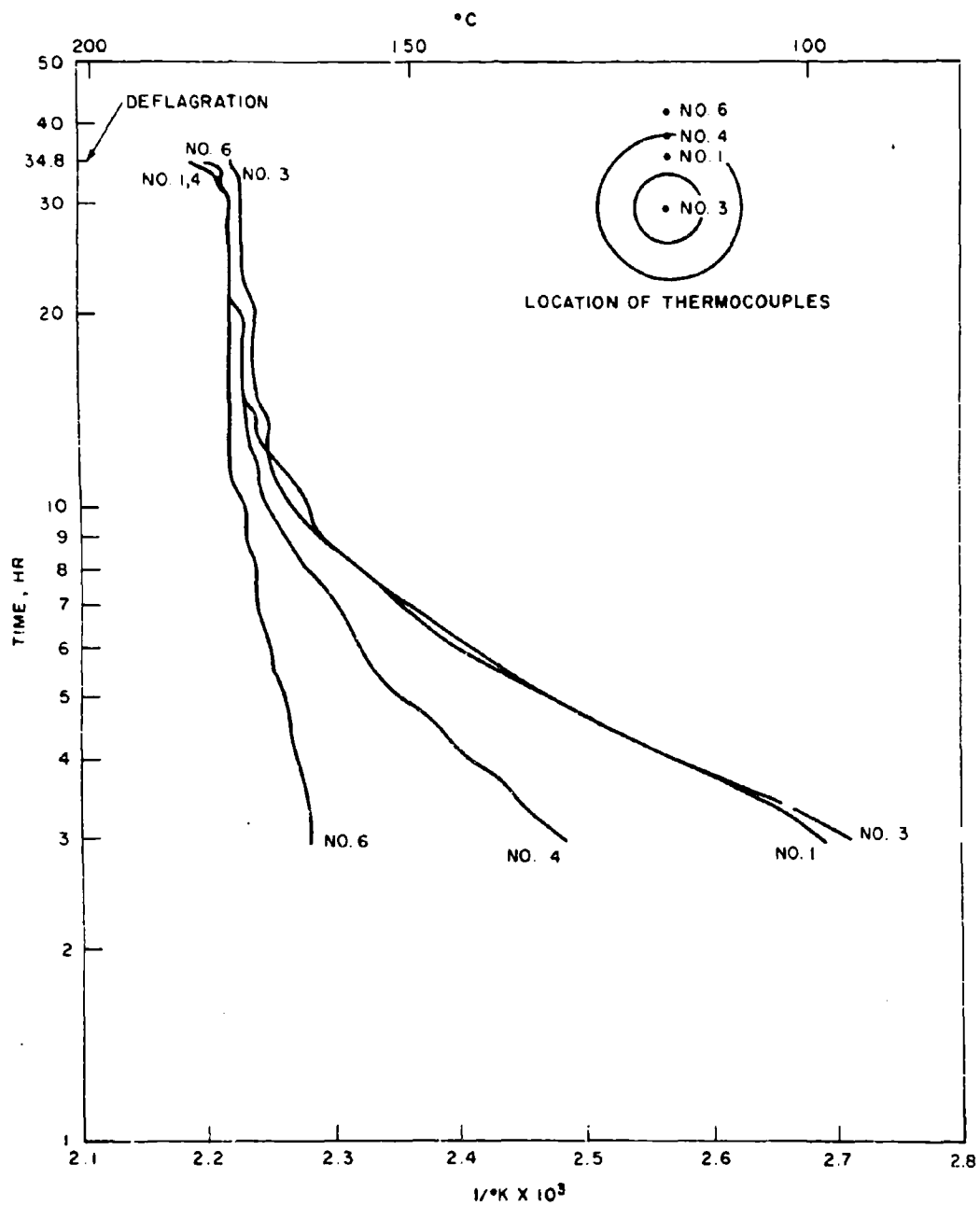
Fig. 6. Thermal Profile for a 5-Inch Diameter x 12.5-Inch Long
Tubular Cylinder of JPL Propellant (BD 68/2) in a
176.7°C Oven.
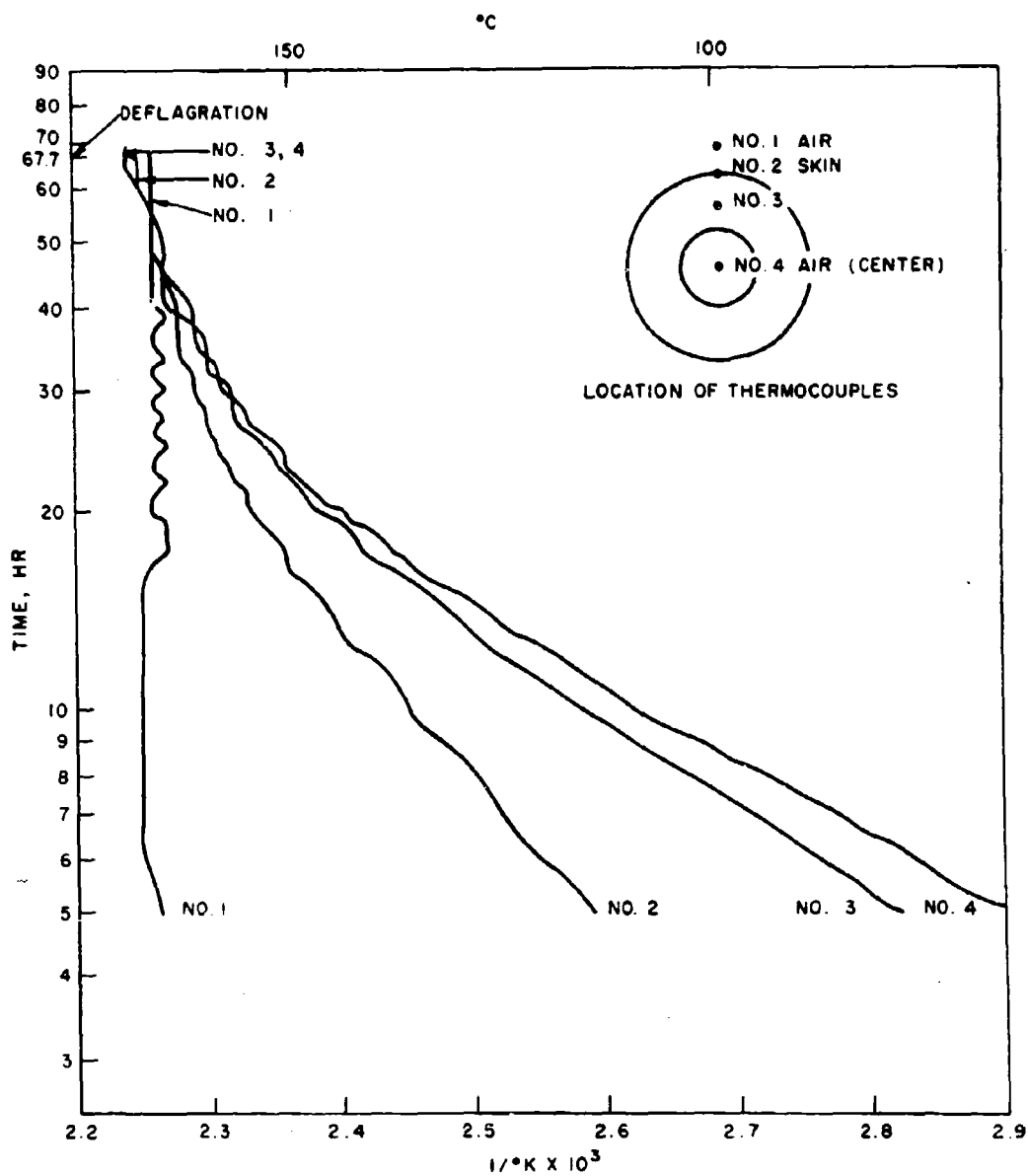
FIG. 7. Thermal Profile for a 10-Inch Diameter x 25-Inch Long
Tubular Cylinder of JPL Propellant (BD 82/6) in a
168.9°C Oven.

27
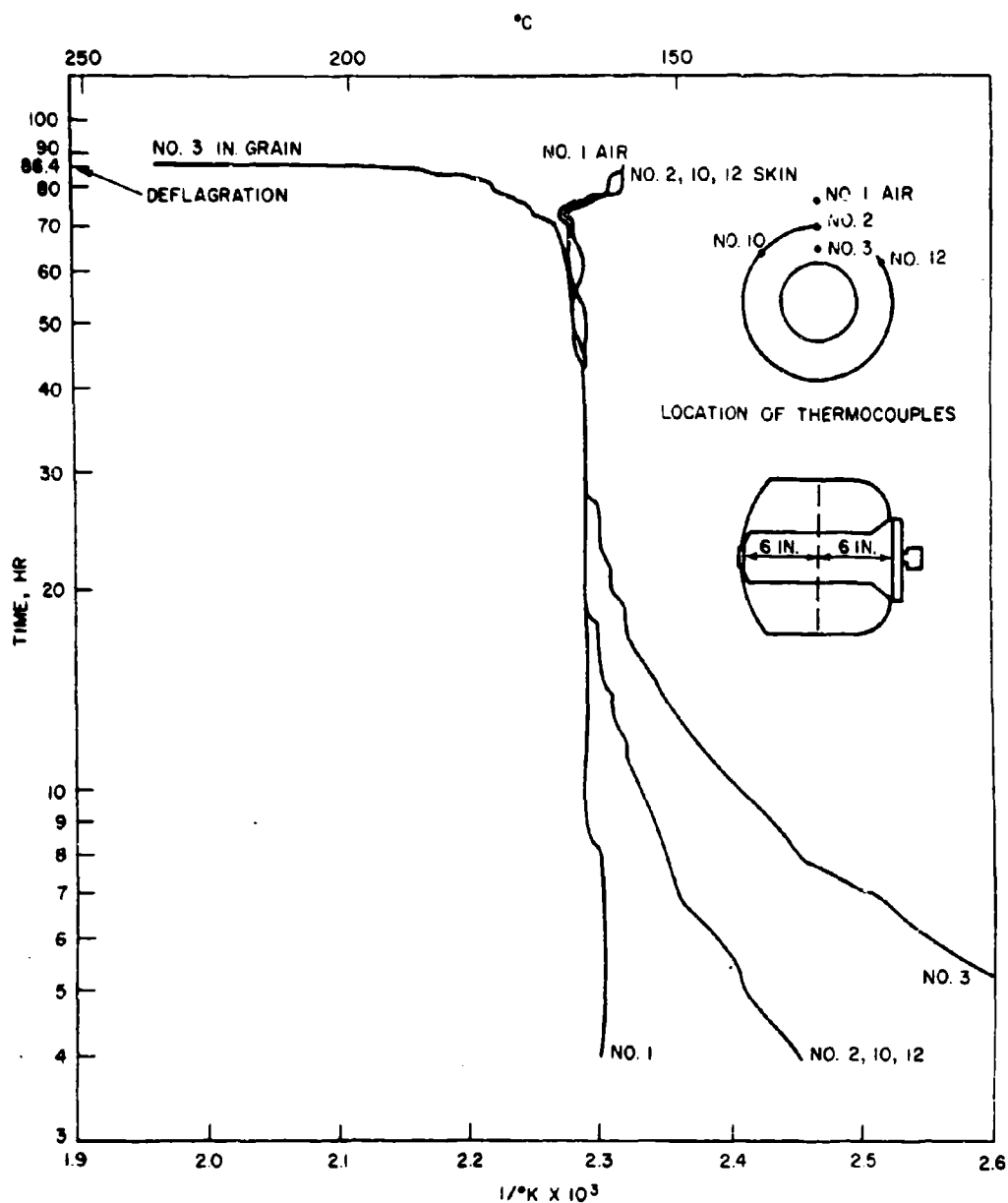
FIG. 8. Thermal Profile for a 12-Inch Diameter (d/D = 1/2)
Motor With JPL Propellant in a 163.3°C Oven.
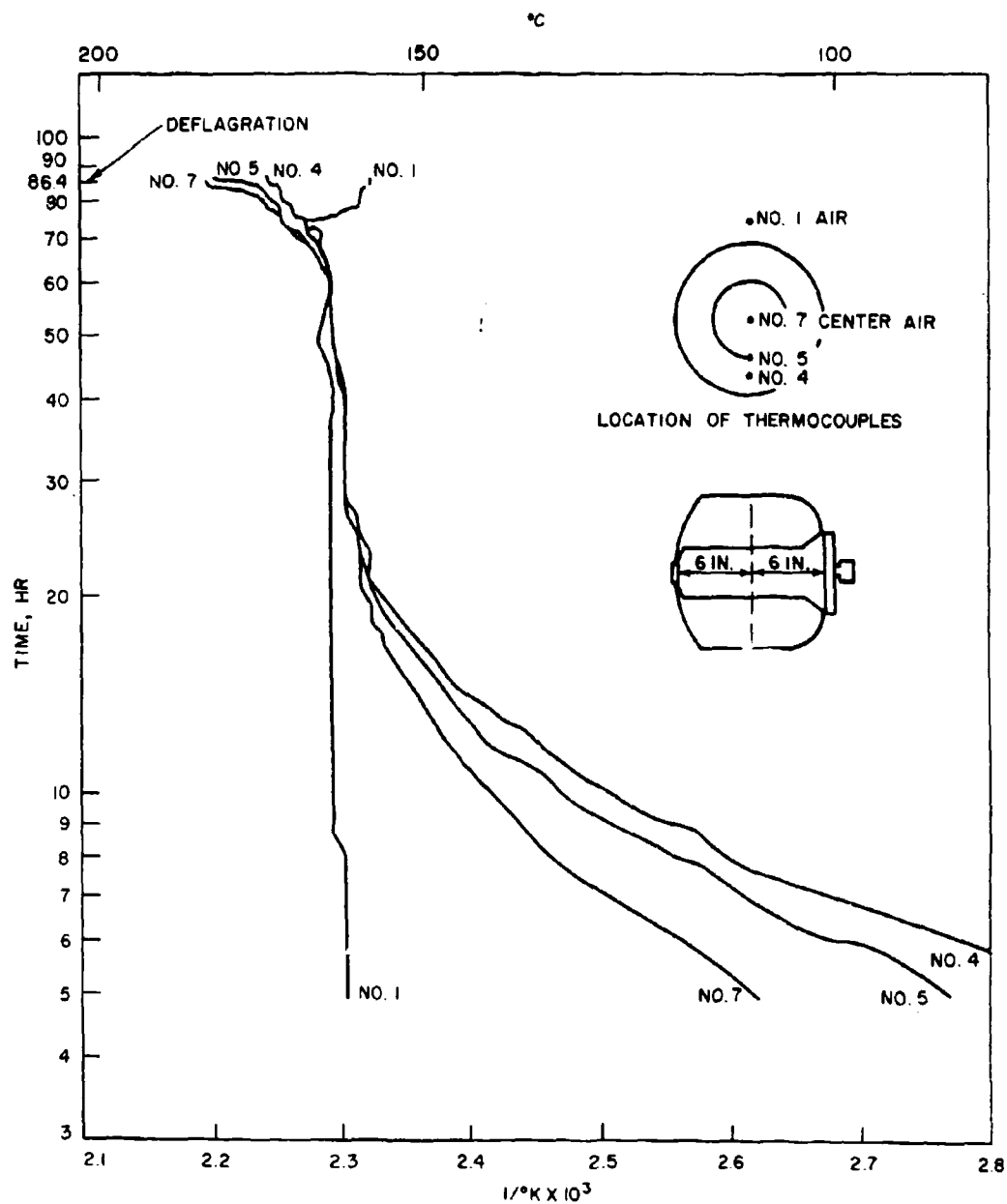
FIG. 9. Thermal Profile for a 12-Inch Diameter (d/D = 1/2)
Motor With JPL Propellant in a 163.3°C Oven.
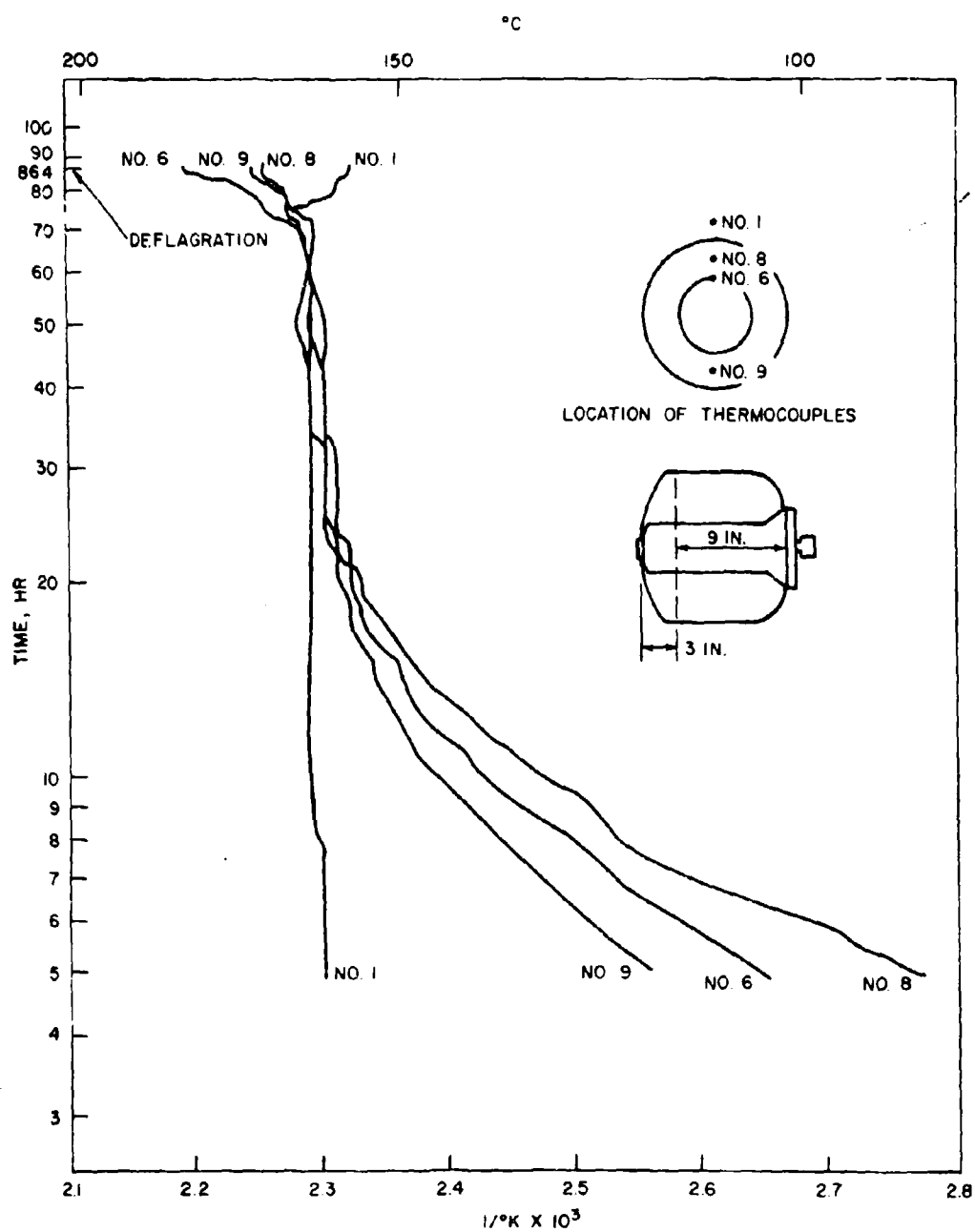
FIG. 10.   Thermal Profile for a 12-Inch Diameter (d/D = 1/2)
Motor With JPL Propellant in a 163.3°C Oven.
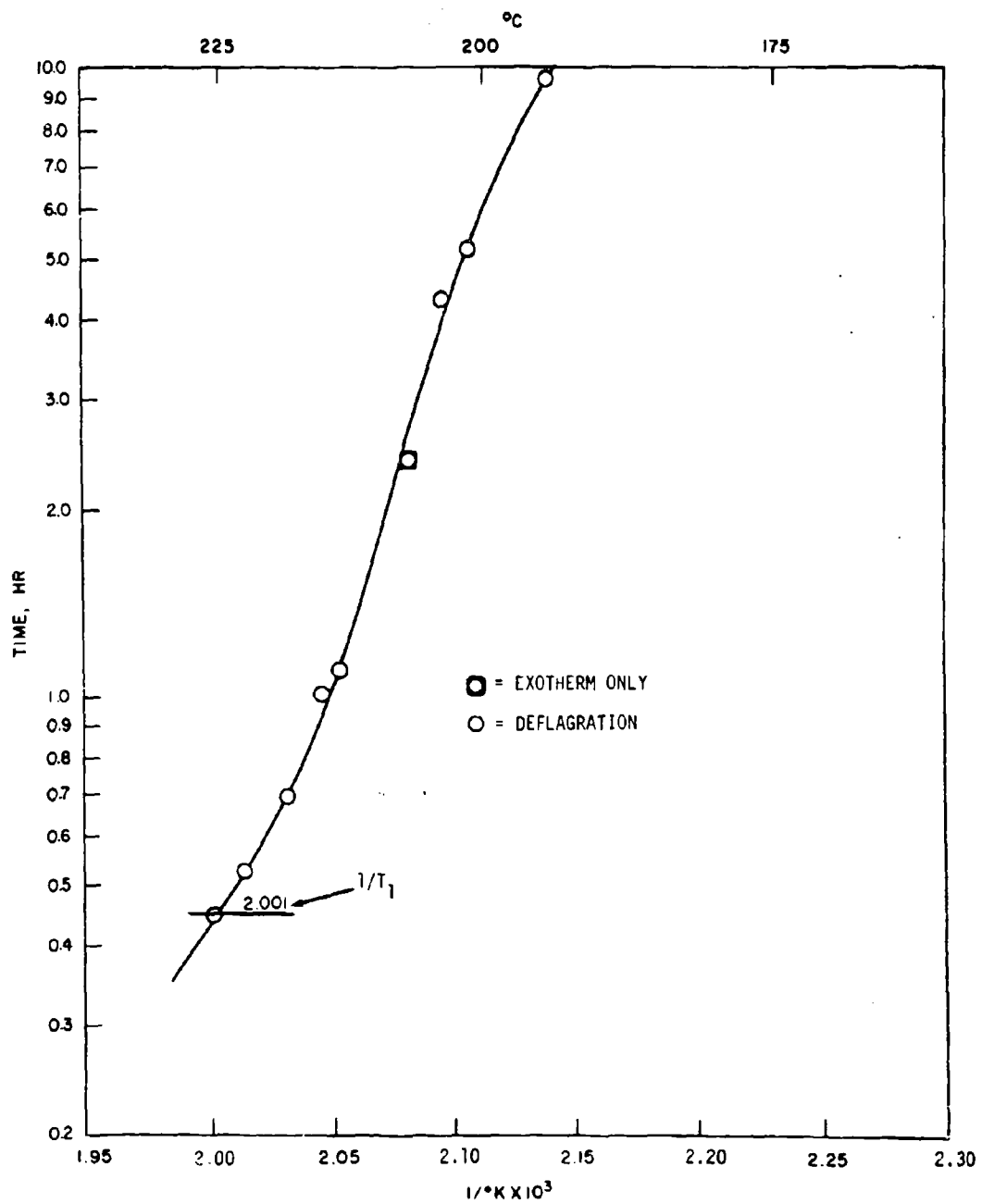
FIG. 11.   Plot of Deflagration Data on 1-Inch
Diameter JPL Propellant Grains.
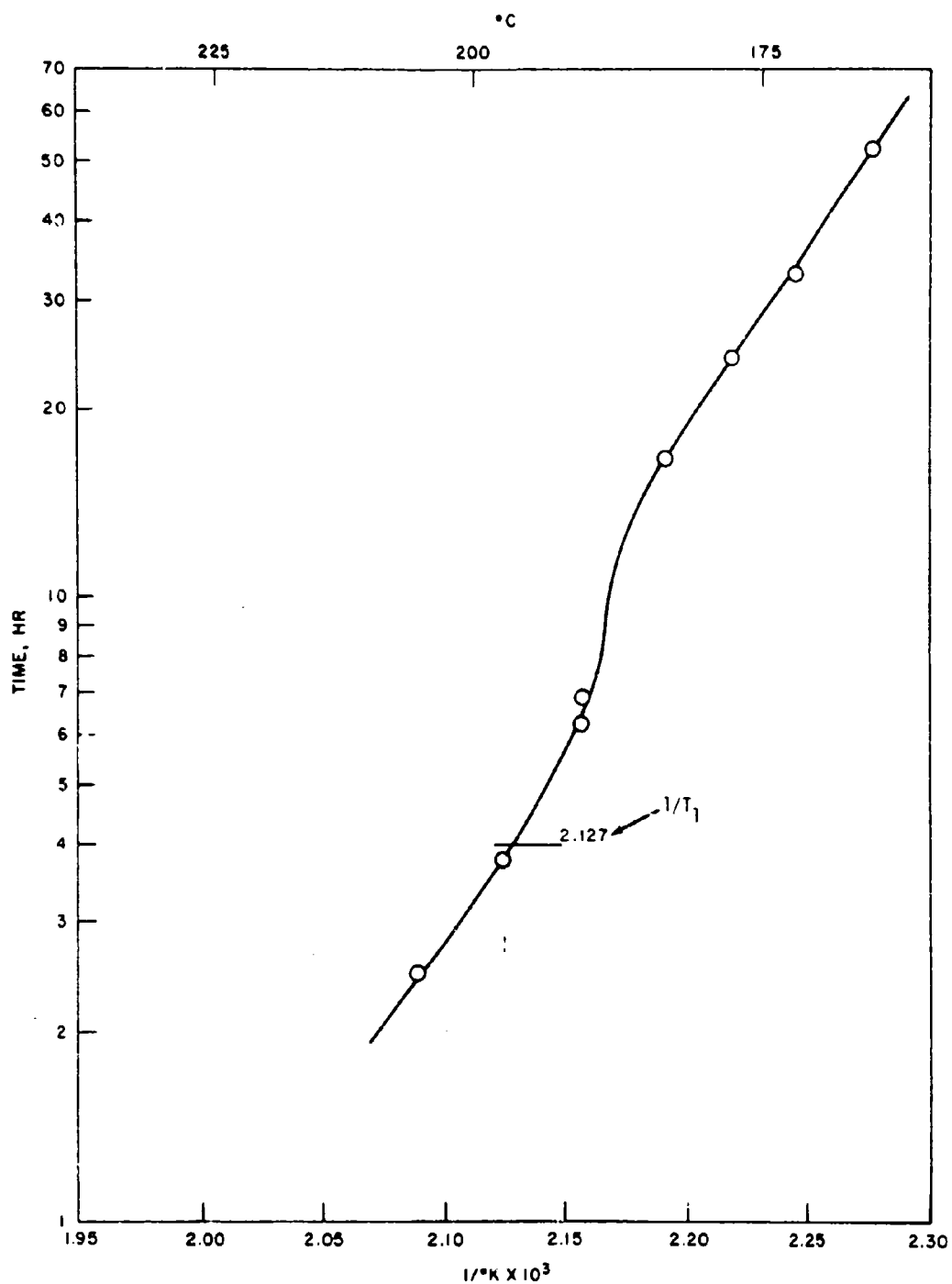
FIG. 12. Plot of Deflagration Data on 3-Inch
Diameter JPL Propellant Grains.
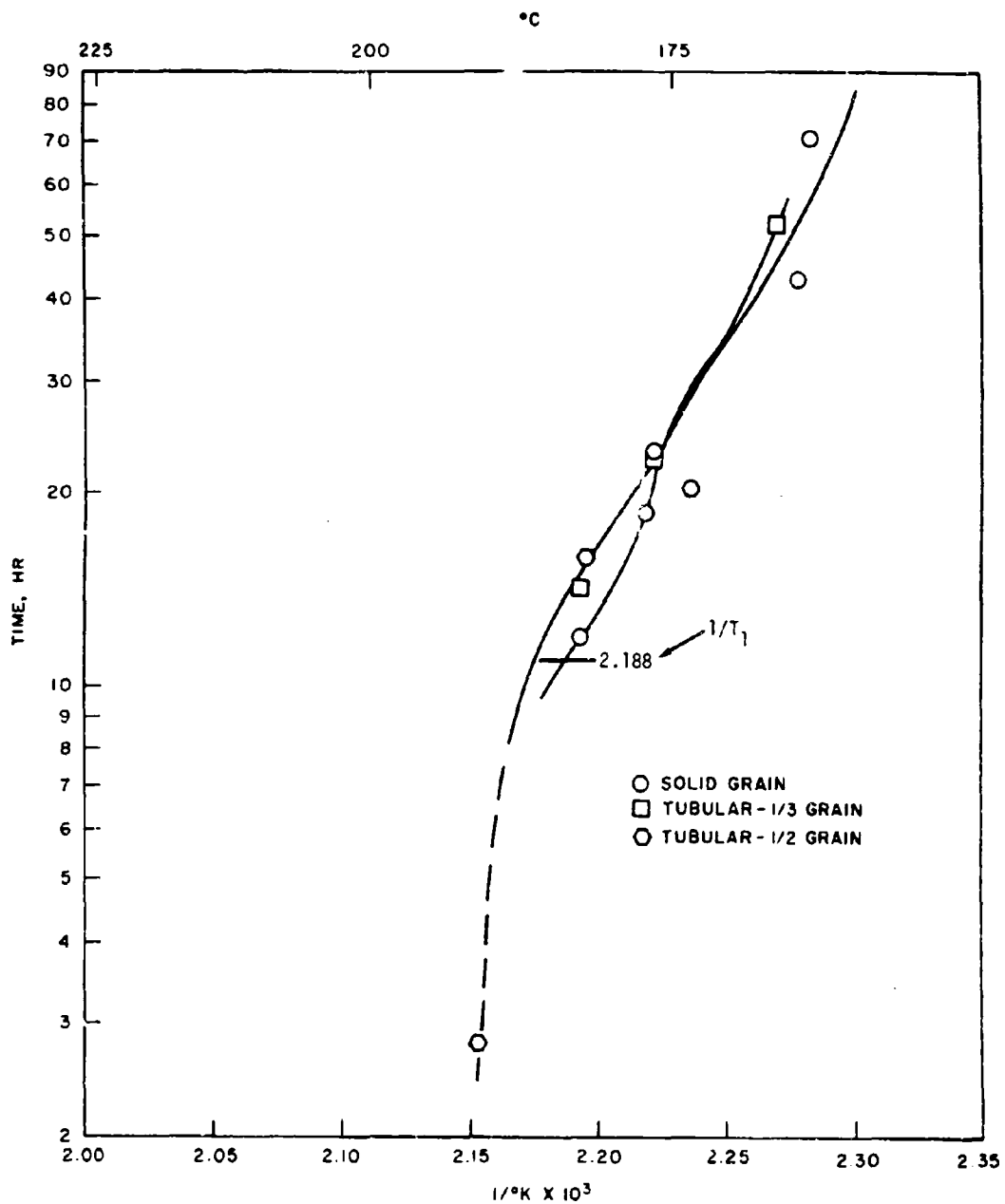
FIG. 13. Plot of Deflagration Data on 5-Inch
Diameter JPL Propellant Grains.
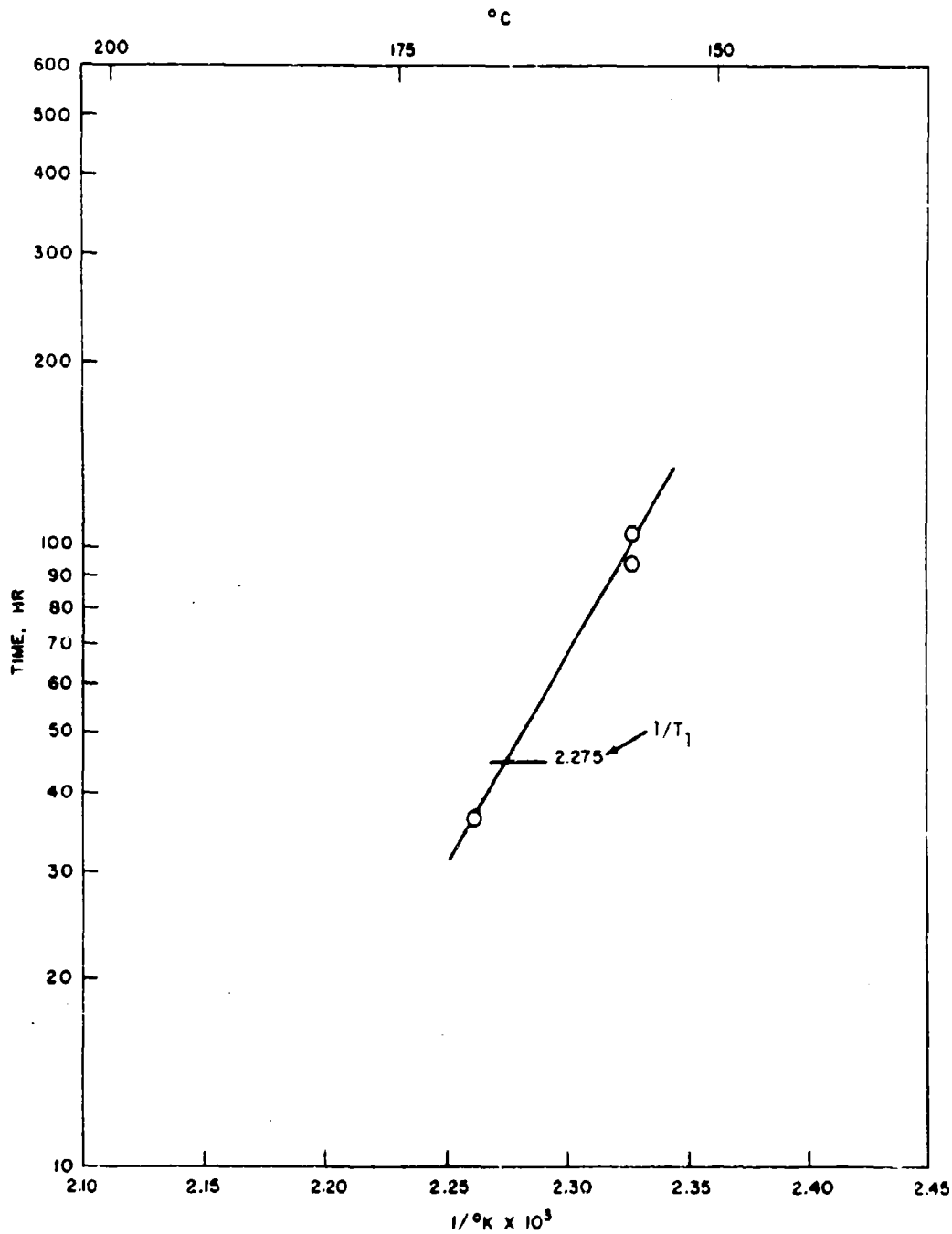
FIG. 14. Plot of Deflagration Data on 10-Inch
Diameter JPL Propellant Grains.
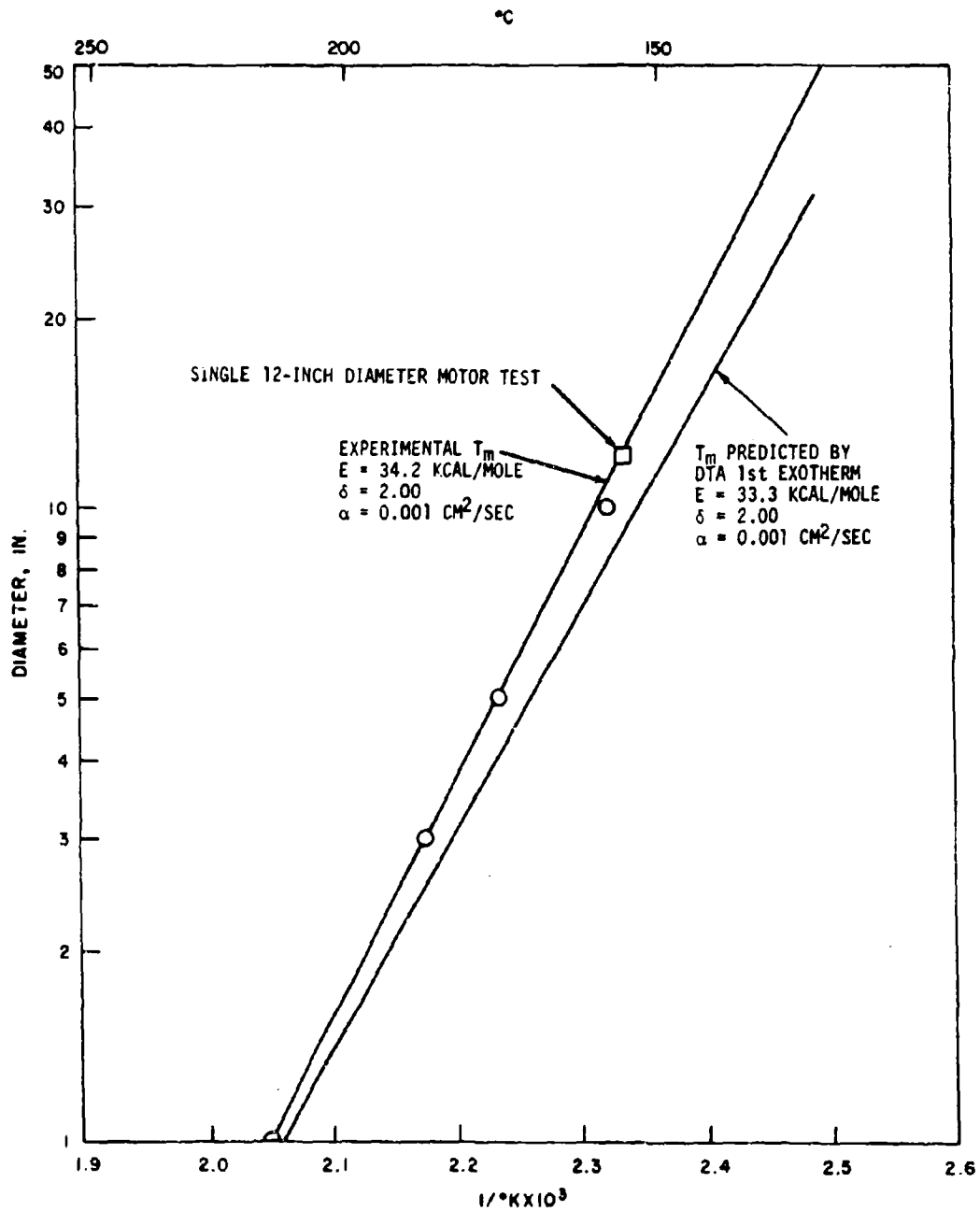
FIG. 15.   Comparison of Predicted and Experimental T_m
for Various Diameters of JPL Propellant
Grains.

35
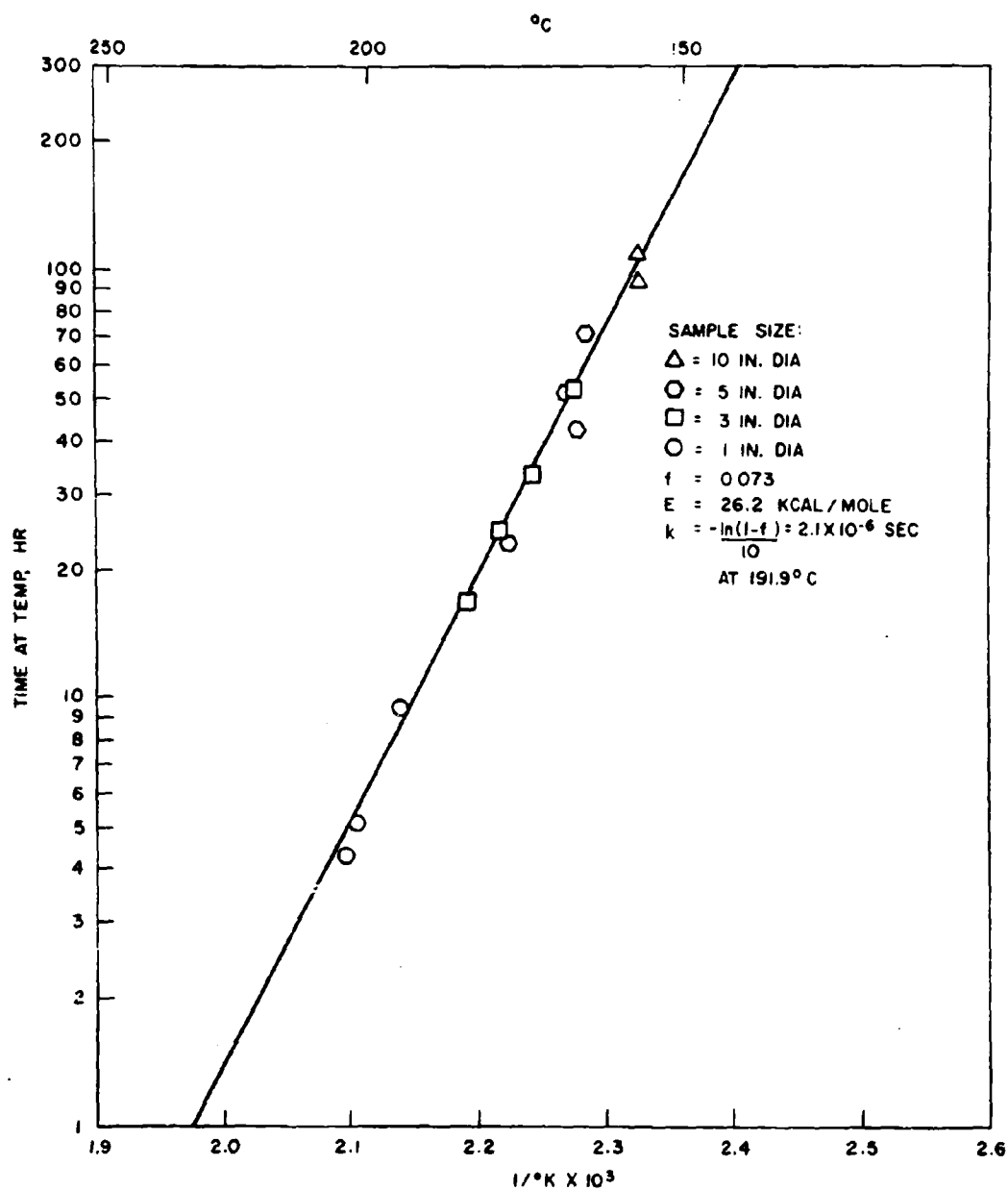
FIG. 16. Deflagration Times Under Isothermal
Conditions Where $T_m > T_1$ for Various
Diameters of JPL Propellant Grains.

36

SAMPLE: JS-1, 2, 3, 7
RUN NO.: 723
HEATING RATE: 7° C/MIN

SAMPLE WEIGHT:
NO. 1-JS-1   10.8 mg
NO. 2-JS-2   10.3 mg
NO. 3-JS-3   9.6 mg
NO. 4-JS-7   10.9 mg

NO. 1
NO. 2
NO. 3
NO. 4

250   300   350   400   450
°C
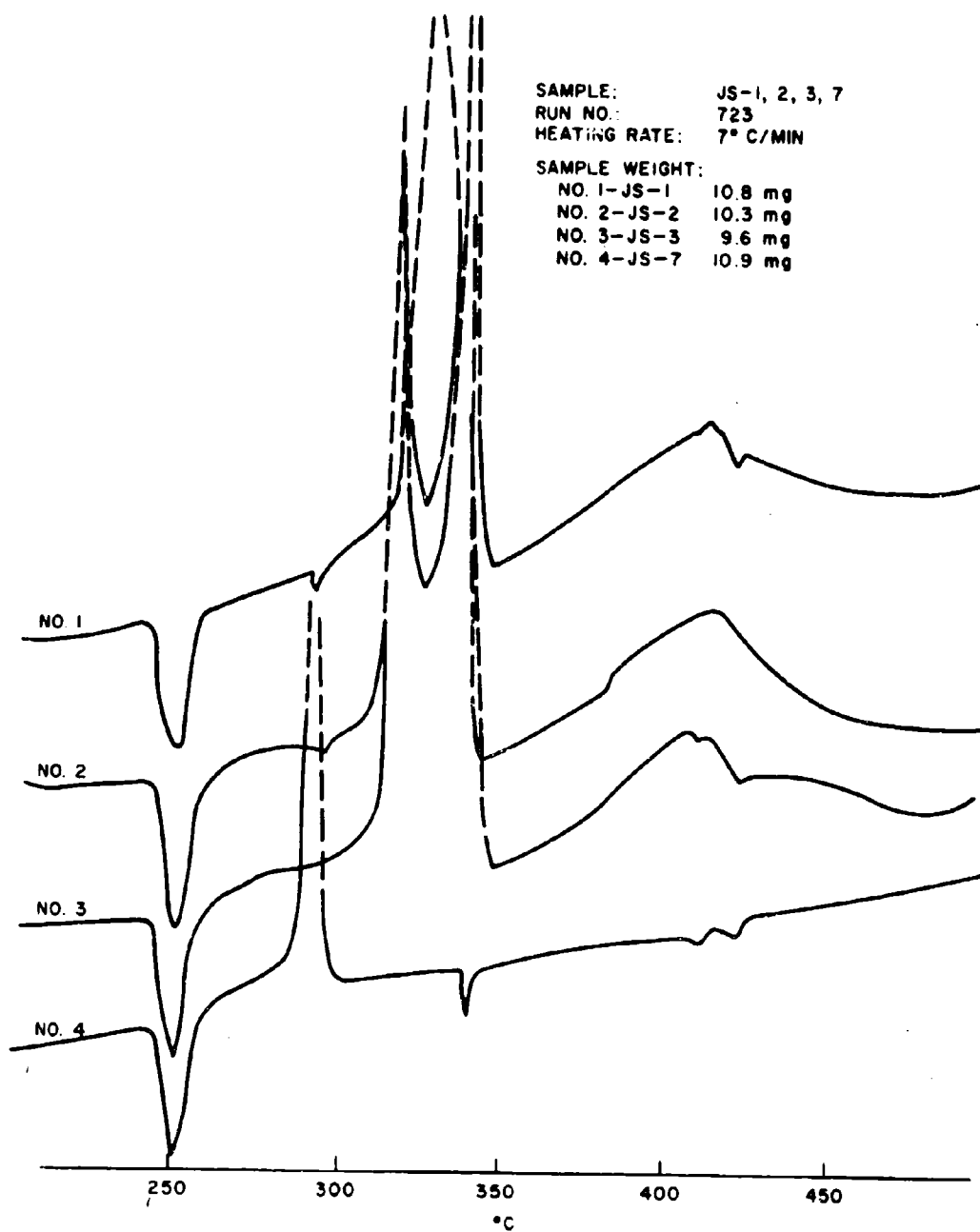
FIG. 17.   DTA Thermal Patterns for Four Different
Batches of JPL Propellant.

SAMPLE : JS-1
RUN NO.: 5-10-2
HEATING RATE : 1°C/MIN
WEIGHT : 37.3 mg

FIG. 18.   DTA Thermal Pattern for JPL Propellant, Batch JS-1.

SAMPLE: JS-1
RUN NO.: 5-6-6
HEATING RATE: 2.94 °C/MIN
WEIGHT: 23.2 mg

FIG. 19. DTA Thermal Pattern for JPL Propellant, Batch JS-1.

39

SAMPLE: JS-1
RUN NO.:   5-7-3
HEATING RATE: 7.1 °C/MIN
WEIGHT: 18.8 mg

FIG. 20.   DTA Thermal Pattern for JPL Propellant, Batch JS-1.

SAMPLE: JS-2
RUN NO.: 4-55-2
HEATING RATE: 0.83°C/MIN
WEIGHT: 21.8 mg
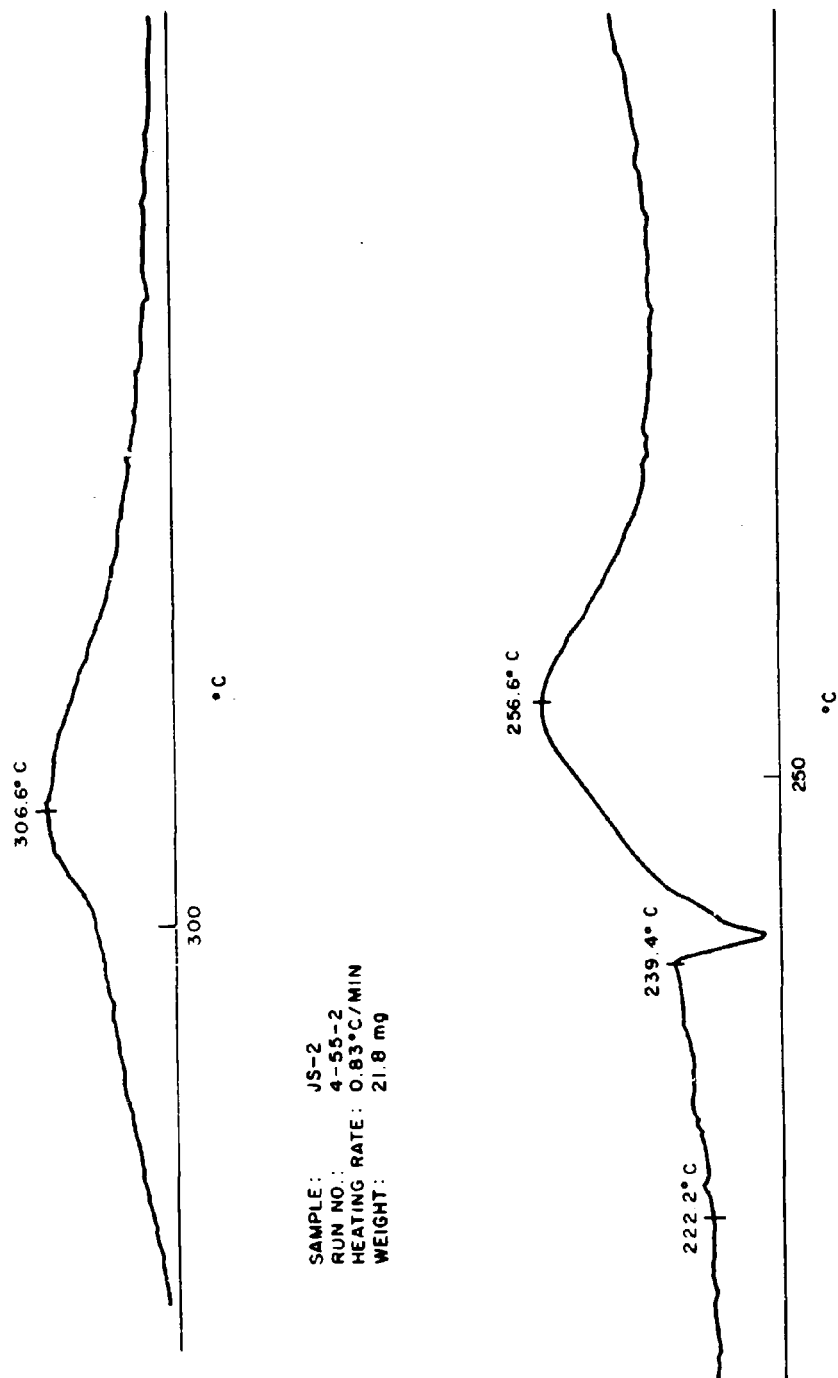
FIG. 21. DTA Thermal Pattern for JPL Propellant, Batch JS-2.

41
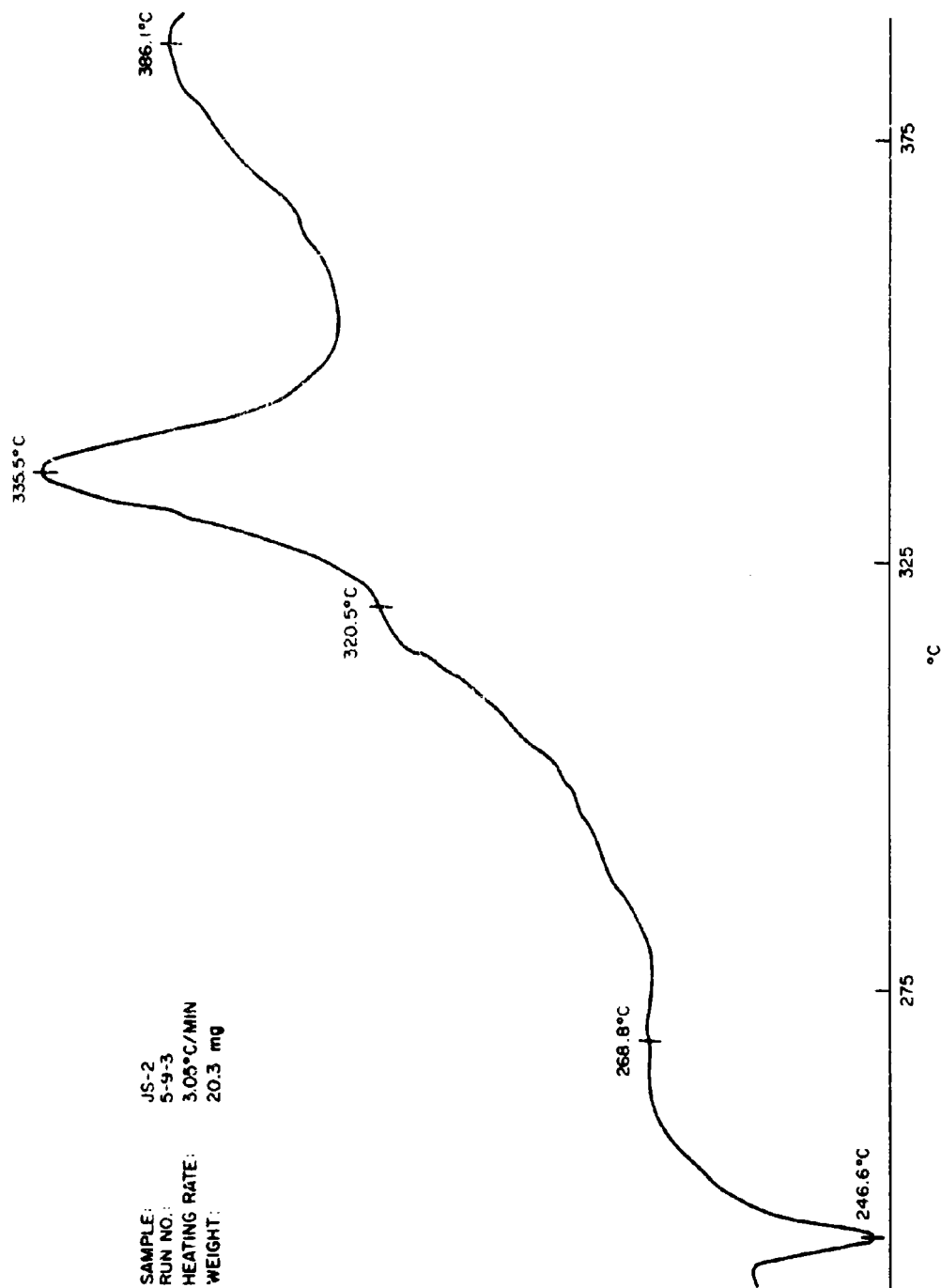
FIG. 22. DTA Thermal Pattern for JPL Propellant, Batch JS-2.

SAMPLE: JS-2
RUN NO: 5-9-3
HEATING RATE: 3.05°C/MIN
WEIGHT: 20.3 mg

366.1°C

335.5°C

320.5°C

268.8°C

246.6°C

°C

275   325   375

42

FIG. 23. DTA Thermal Pattern for JPL Propellant, Batch JS-2.
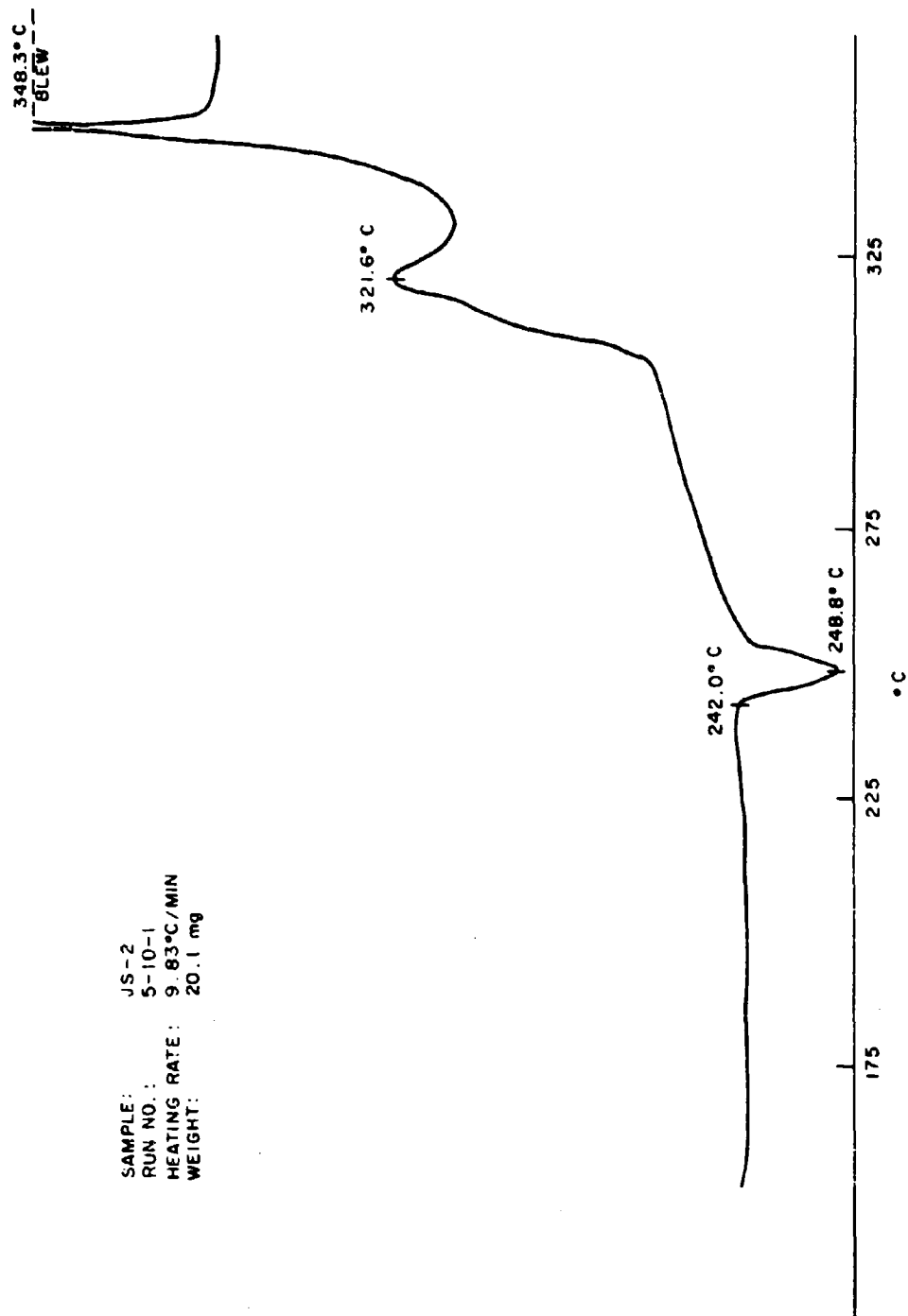
SAMPLE: JS-2
RUN NO.:   5-10-1
HEATING RATE: 9.83°C/MIN
WEIGHT: 20.1 mg

348.3°C
BLEW

321.6°C

242.0°C

248.8°C

175   225   275   325
°C

43

FIG. 24. DTA Thermal Pattern for JPL Propellant, Batch JS-3.

SAMPLE: JS-3
RUN NO.: 4-50-2
HEATING RATE: 1°C/MIN
WEIGHT: 20.5 mg

367.7°C
312.7°C
312.7°C
259.4°C
238.8°C
220°C

350
300
300
250

°C

44
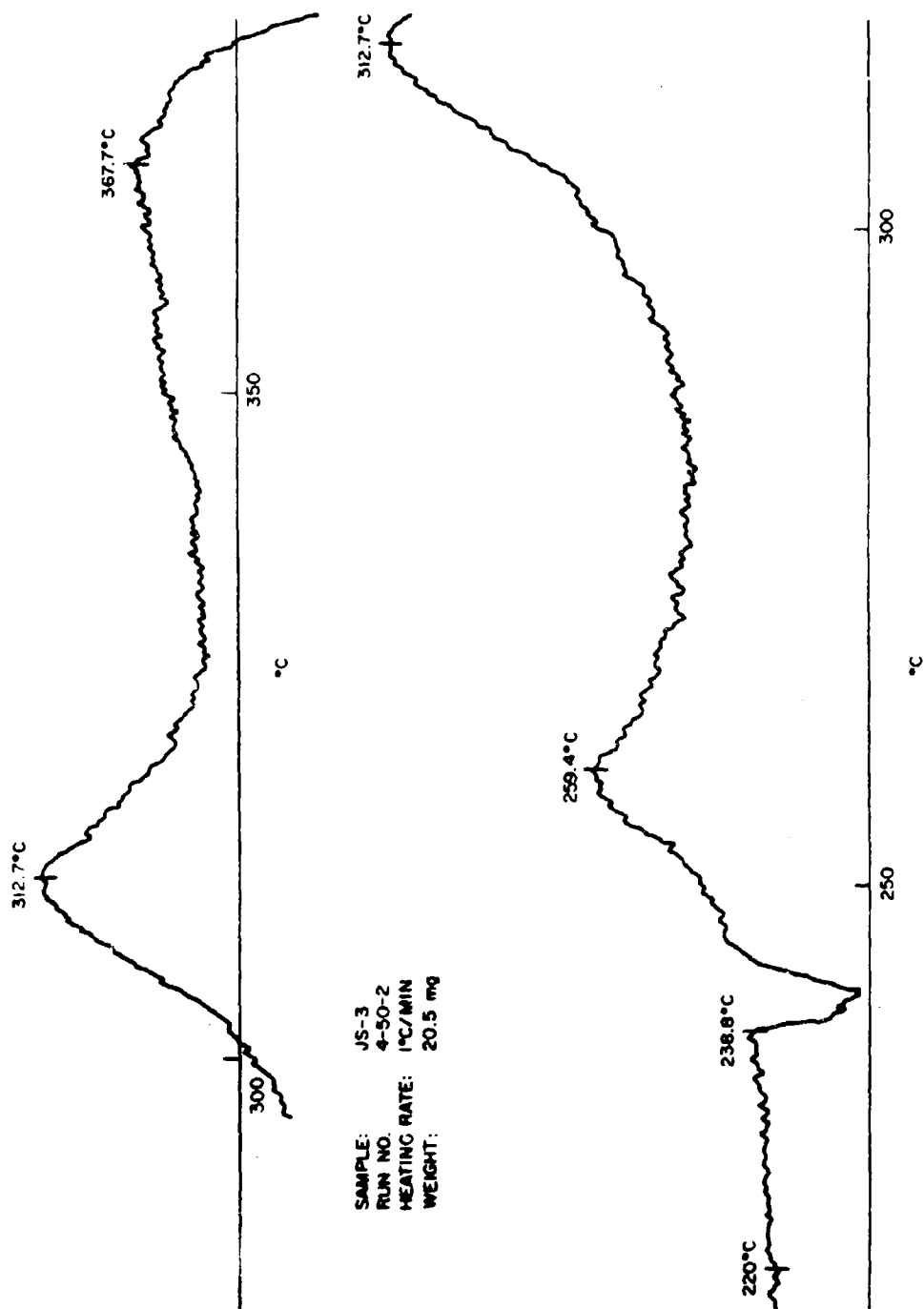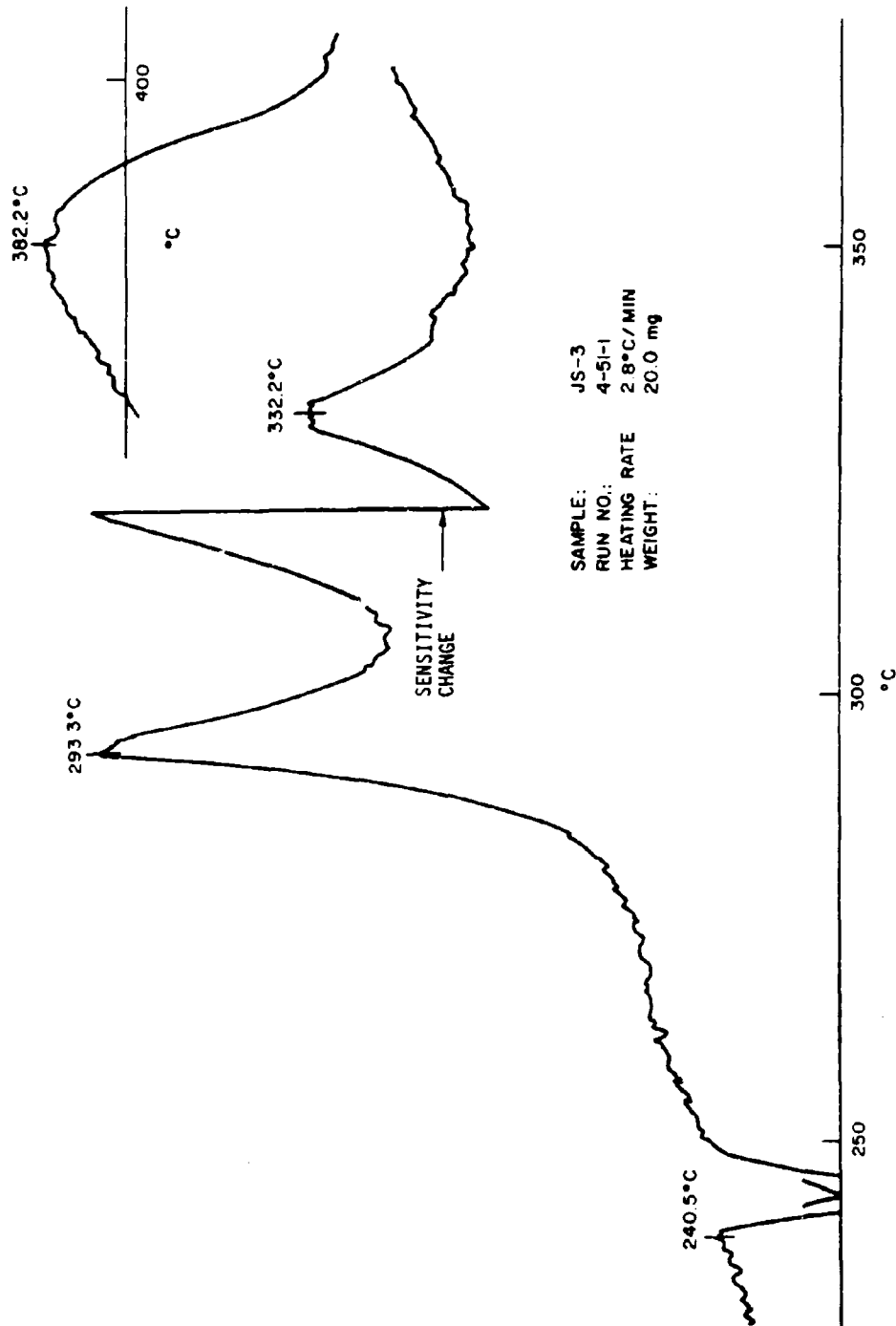
FIG. 25. DTA Thermal Pattern for JPL Propellant, Batch JS-3.

45

FIG. 26. DTA Thermal Pattern for JPL Propellant, Batch JS-3.

SAMPLE: JS-3
RUN NO.: 4-51-2
HEATING RATE: 9.1°C/MIN
WEIGHT: 20.2 mg

FIG. 27. DTA Thermal Pattern for JPL Propellant, Batch JS-7.
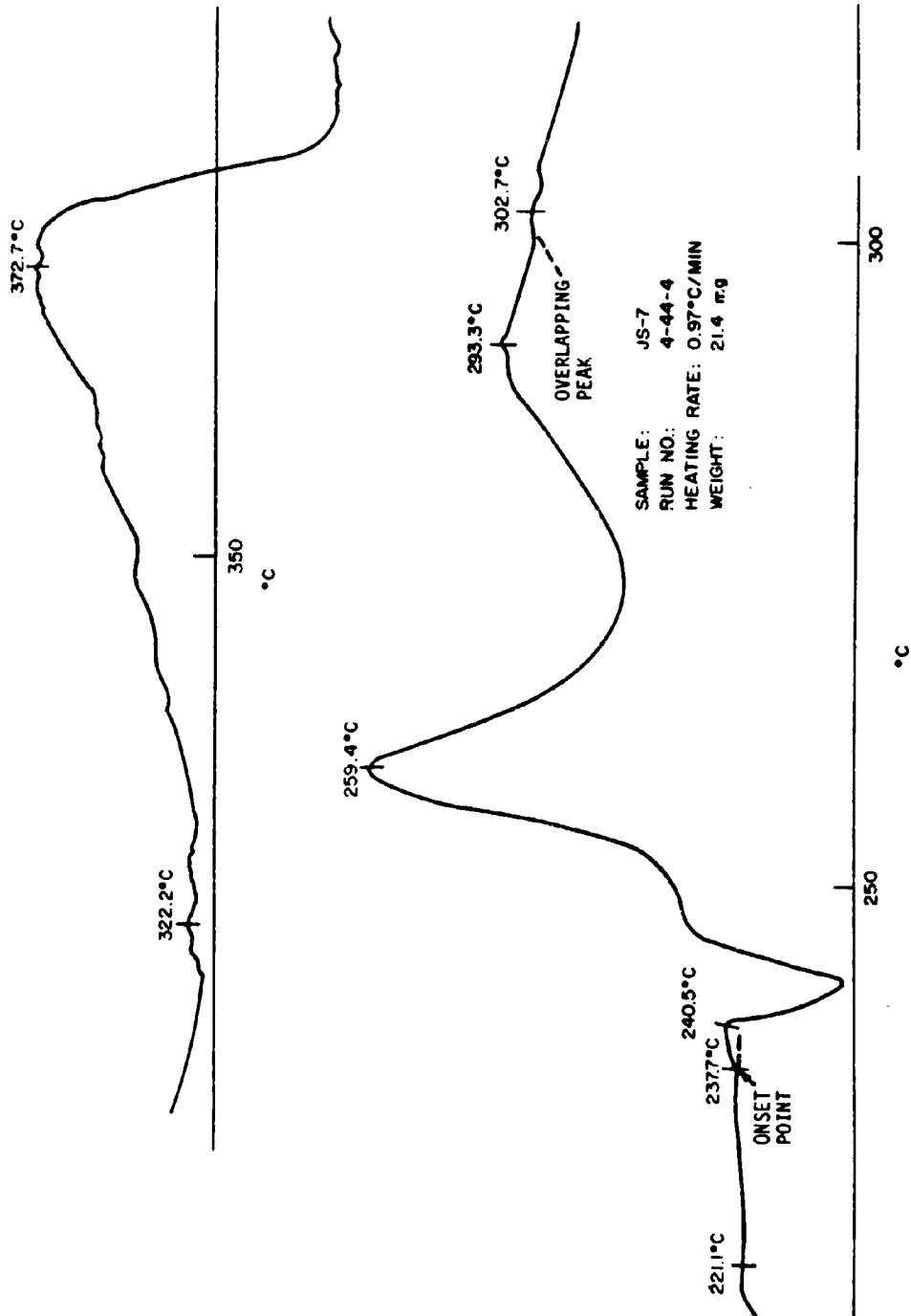
SAMPLE: JS-7
RUN NO.: 4-44-4
HEATING RATE: 0.97°C/MIN
WEIGHT: 21.4 mg

47
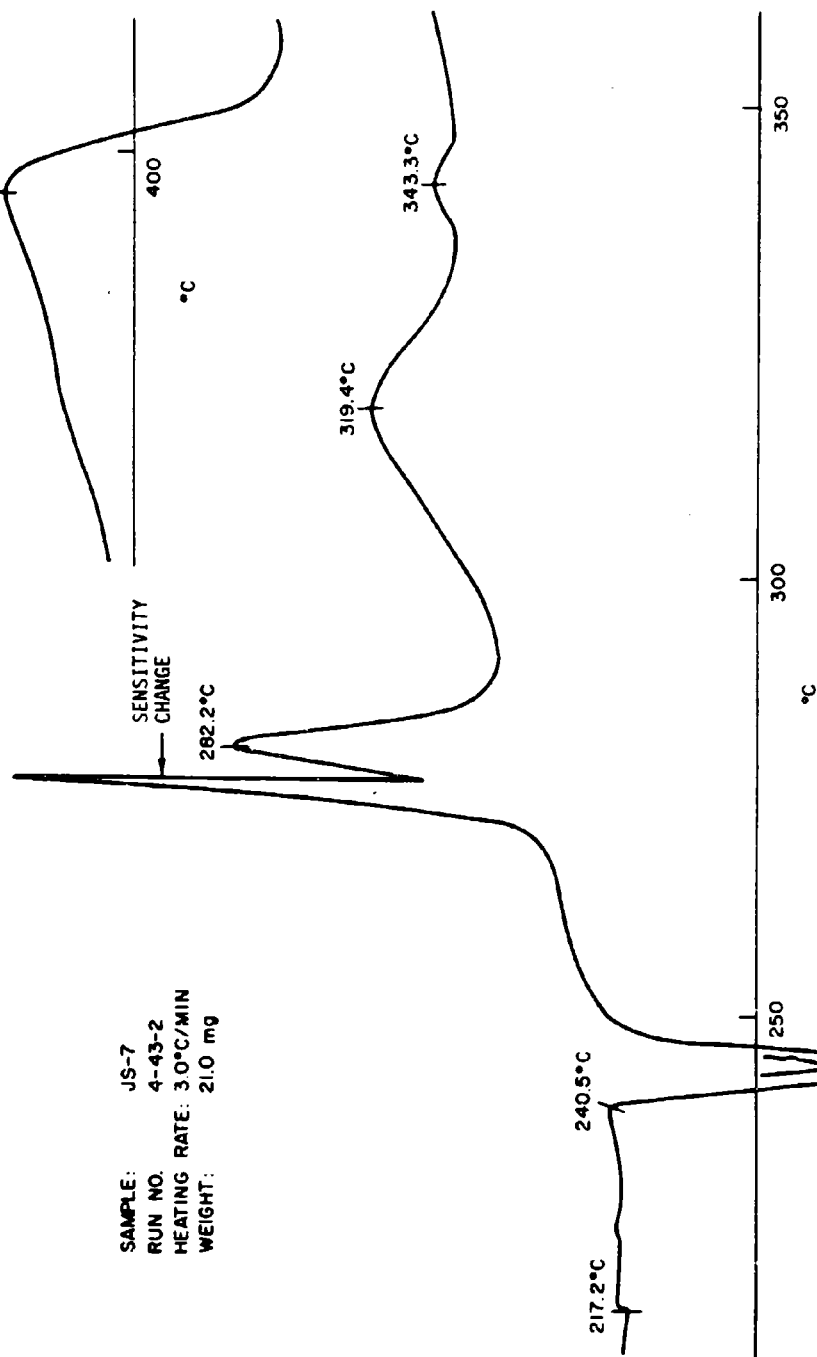
FIG. 28. DTA Thermal Pattern for JPL Propellant, Batch JS-7.

SAMPLE: JS-7
RUN NO. 4-43-2
HEATING RATE: 3.0°C/MIN
WEIGHT: 21.0 mg

SENSITIVITY CHANGE

395.5°C

400

°C

343.3°C

319.4°C

282.2°C

300

°C

350

250

240.5°C

217.2°C

48

SAMPLE: JS-7
RUN NO.: 4-44-1
HEATING RATE: 9.7°C/MIN
WEIGHT: 14.3 mg
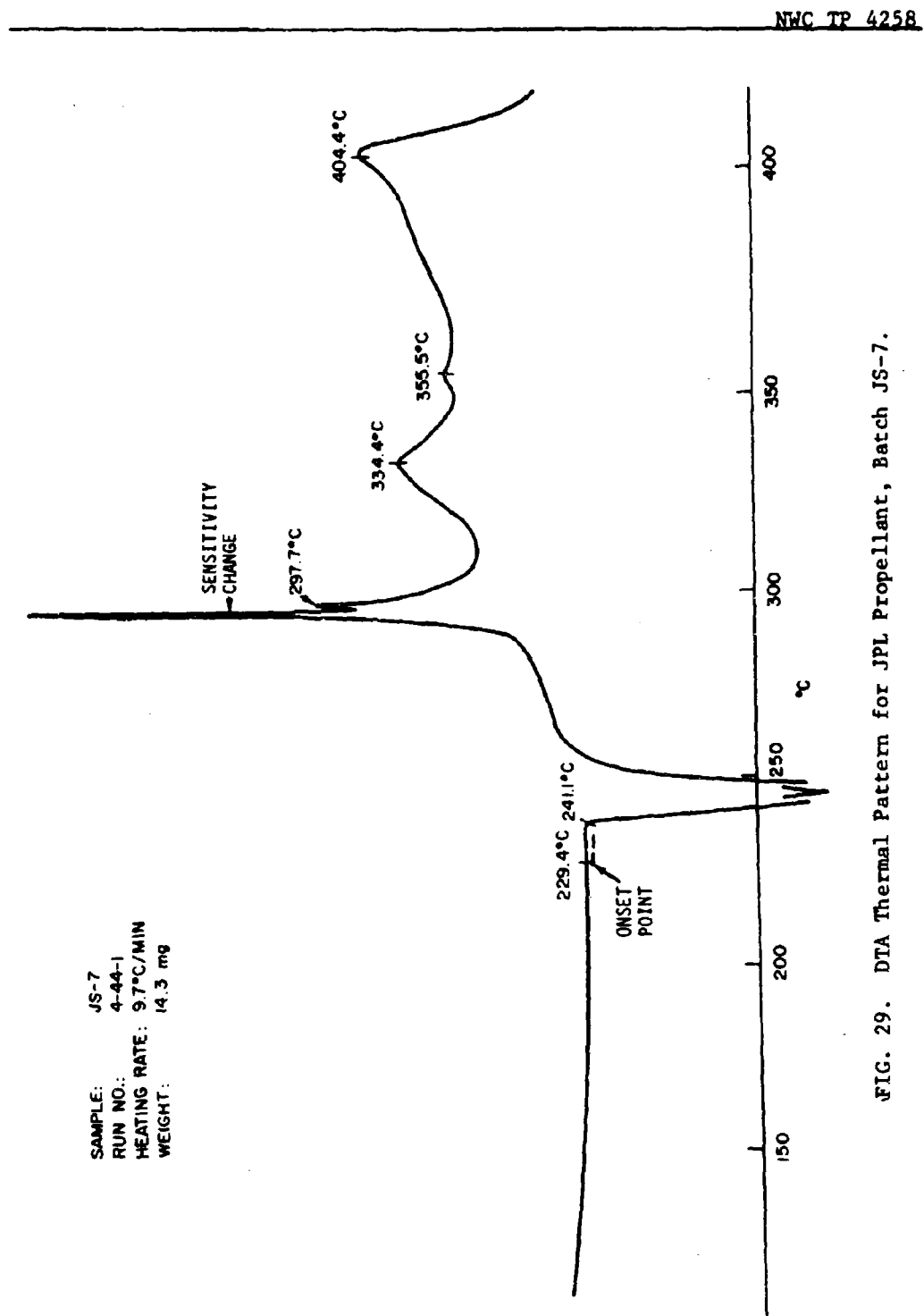
FIG. 29. DTA Thermal Pattern for JPL Propellant, Batch JS-7.
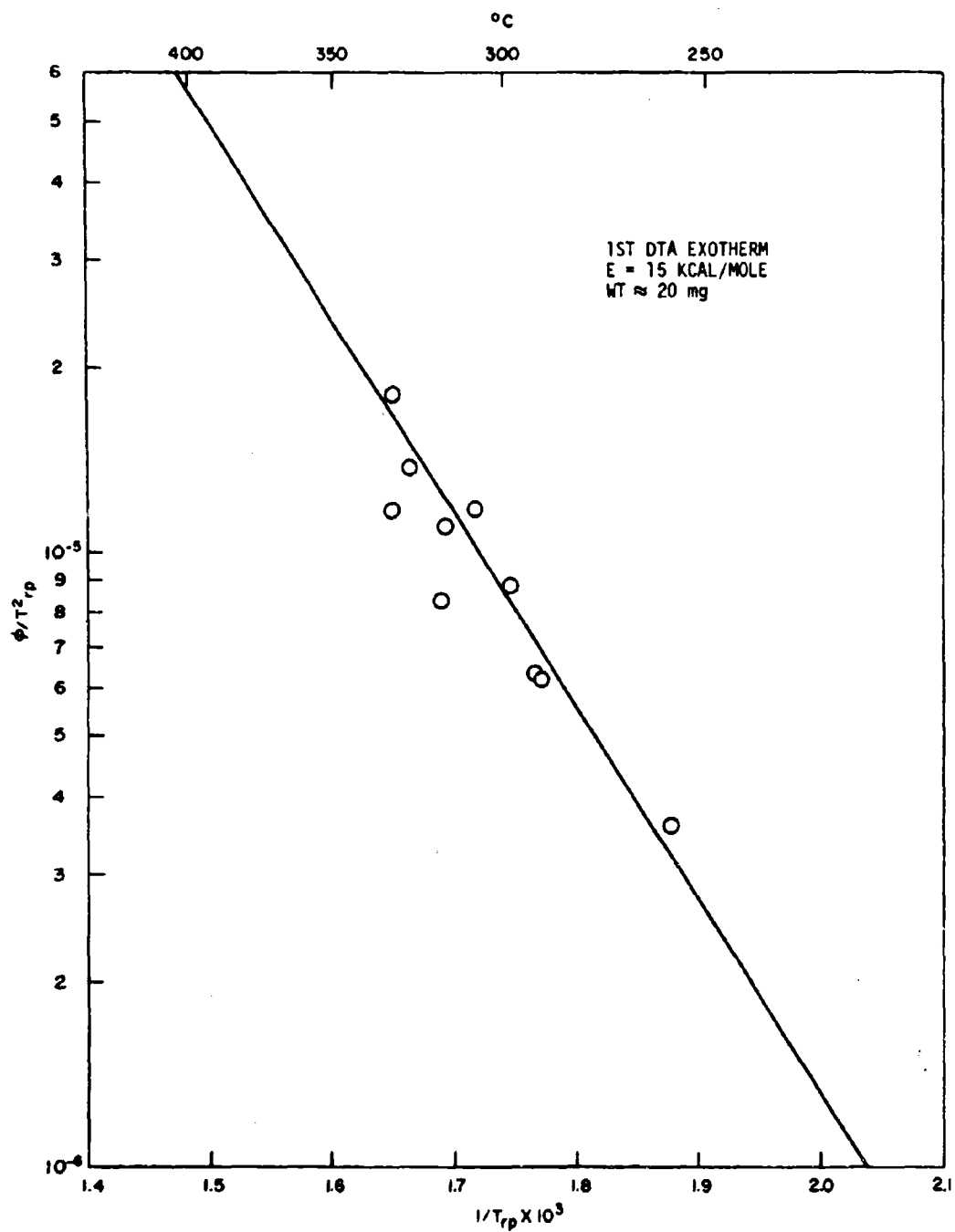
FIG. 30. Plot of DTA Data on JPL Propellant, Batch JS-1.
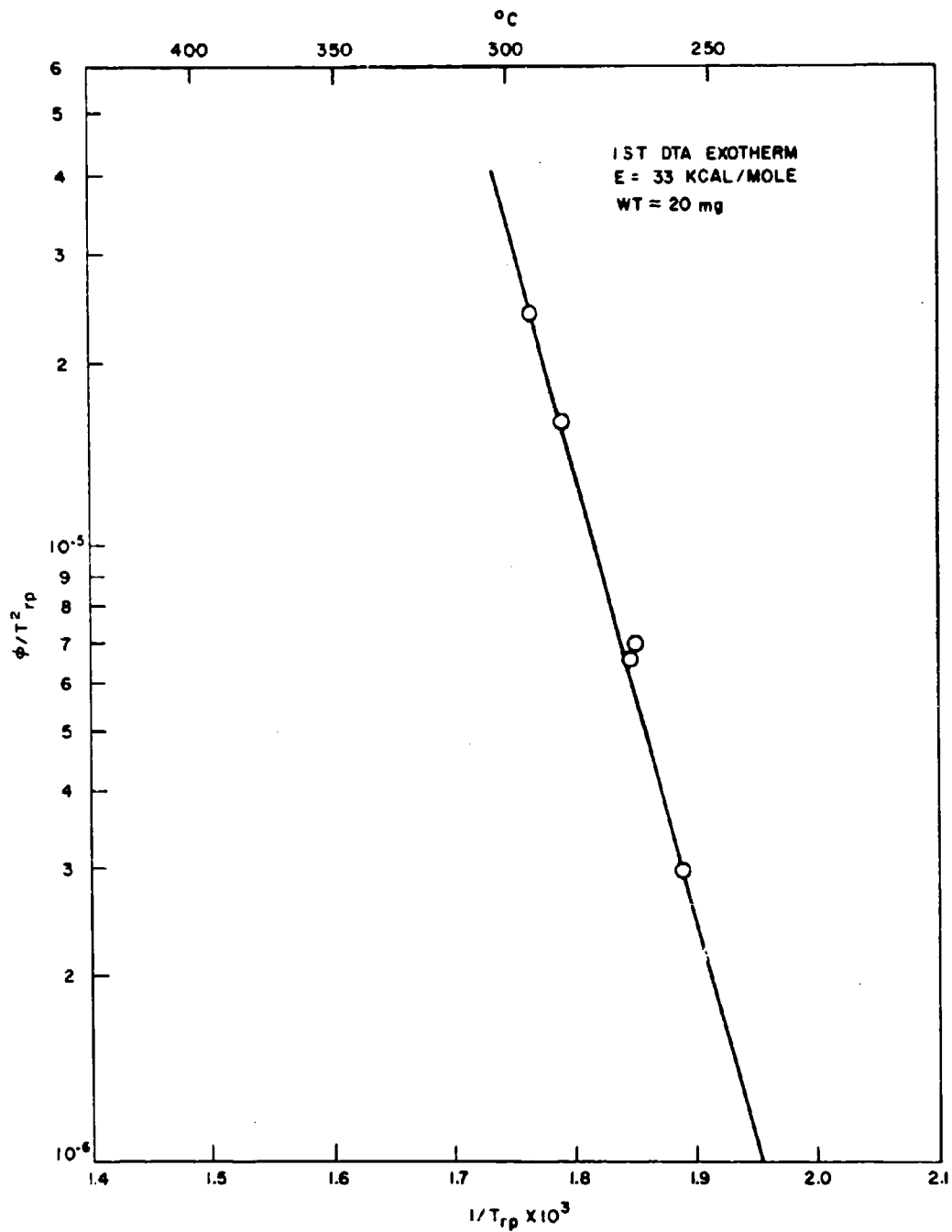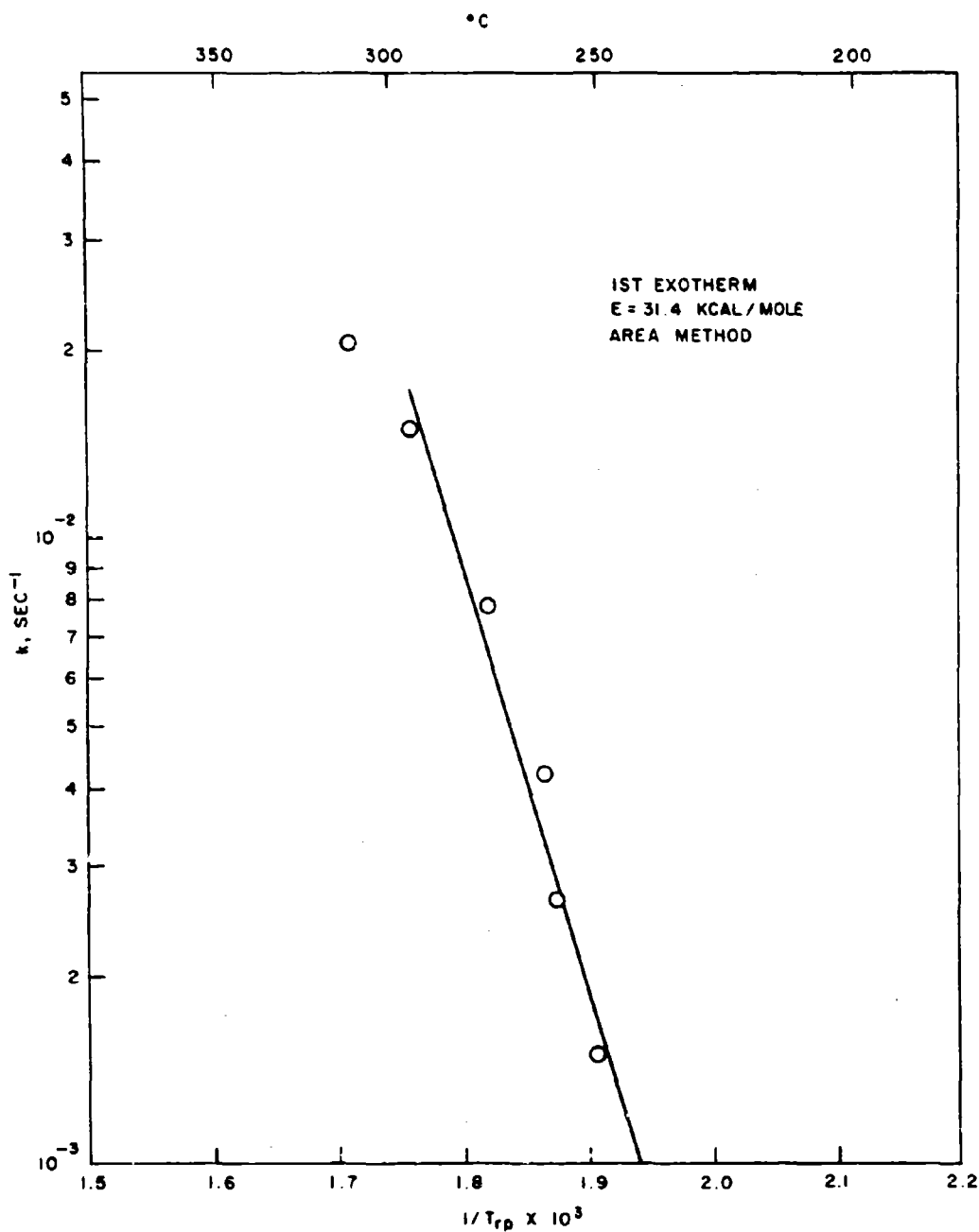
FIG. 31.   Plot of DTA Data on JPL Propellant, Batch JS-2.
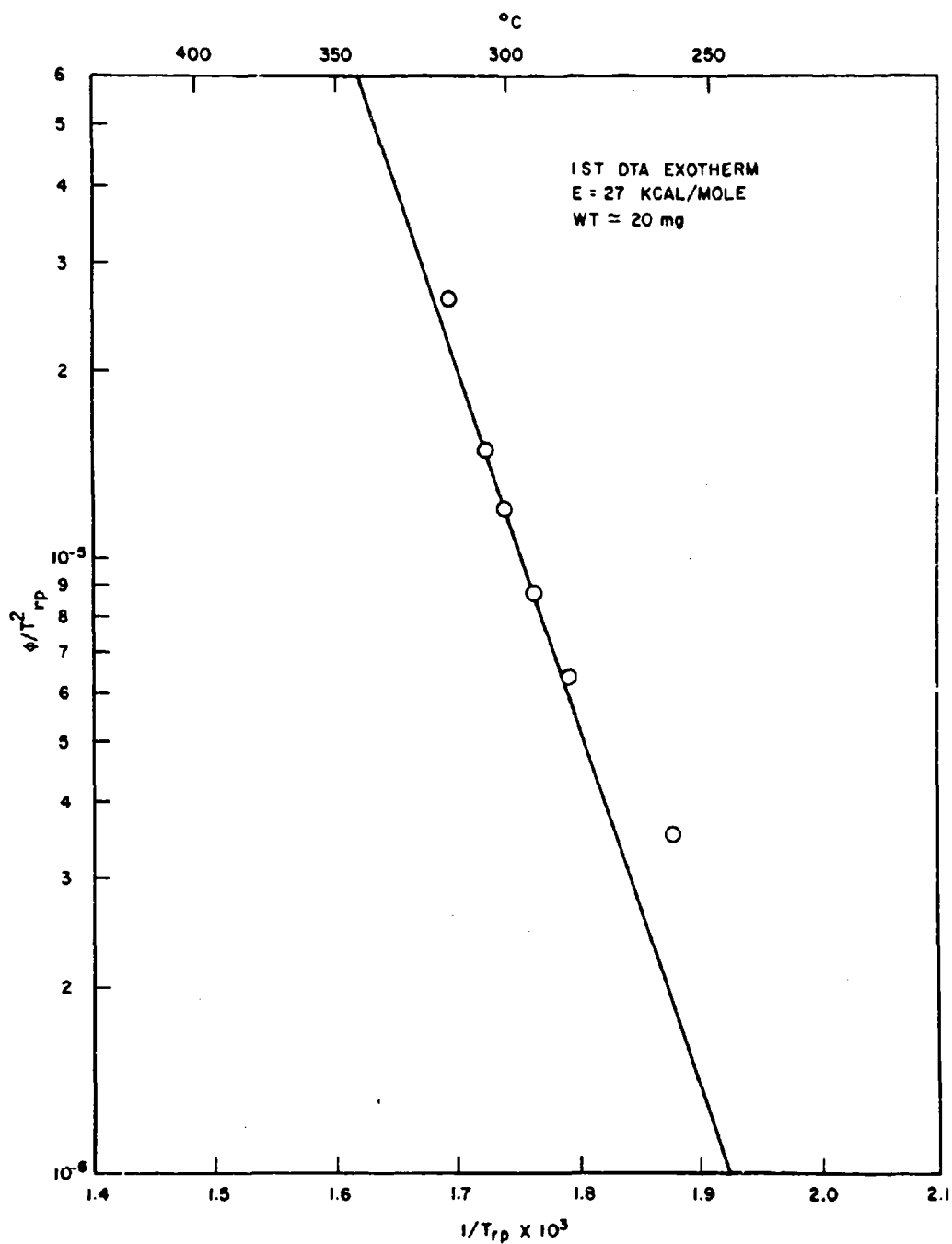
FIG. 32. Plot of DTA Data on JPL Propellant, Batch JS-3.
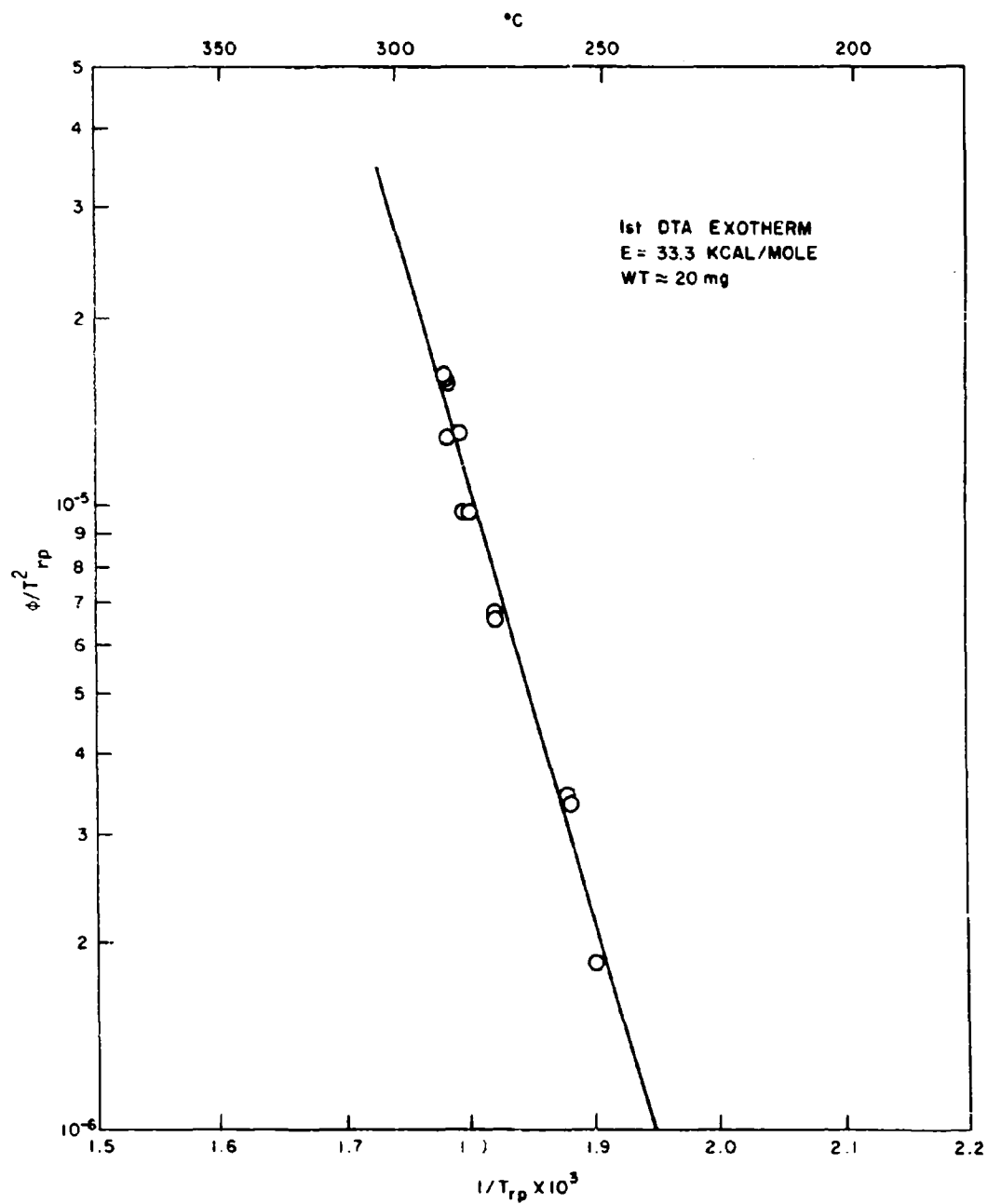
FIG. 33.   Plot of DTA Data on JPL Propellant, Batch JS-7.

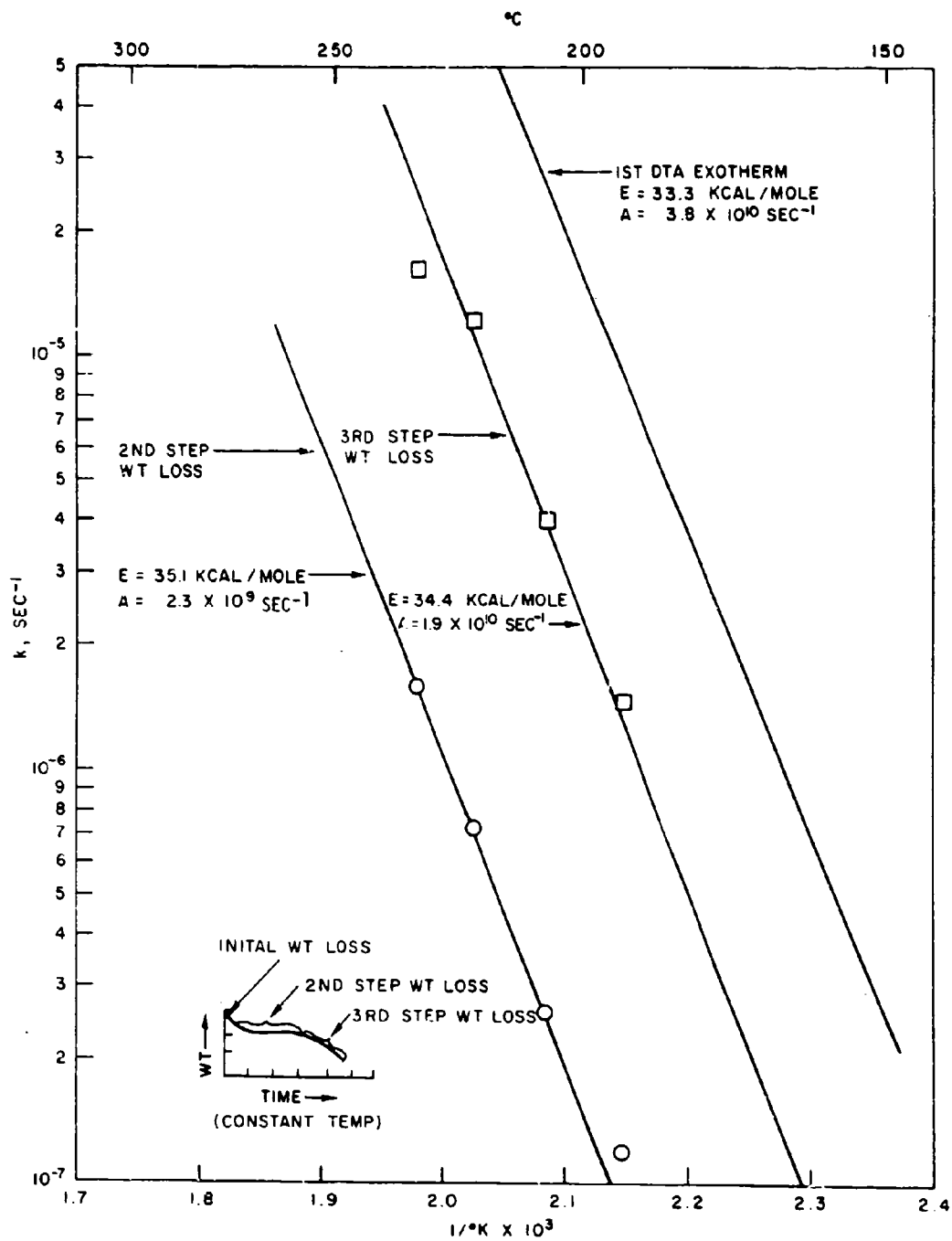FIG. 34. Plot of DTA Data on JPL Propellant, Batch JS-7.

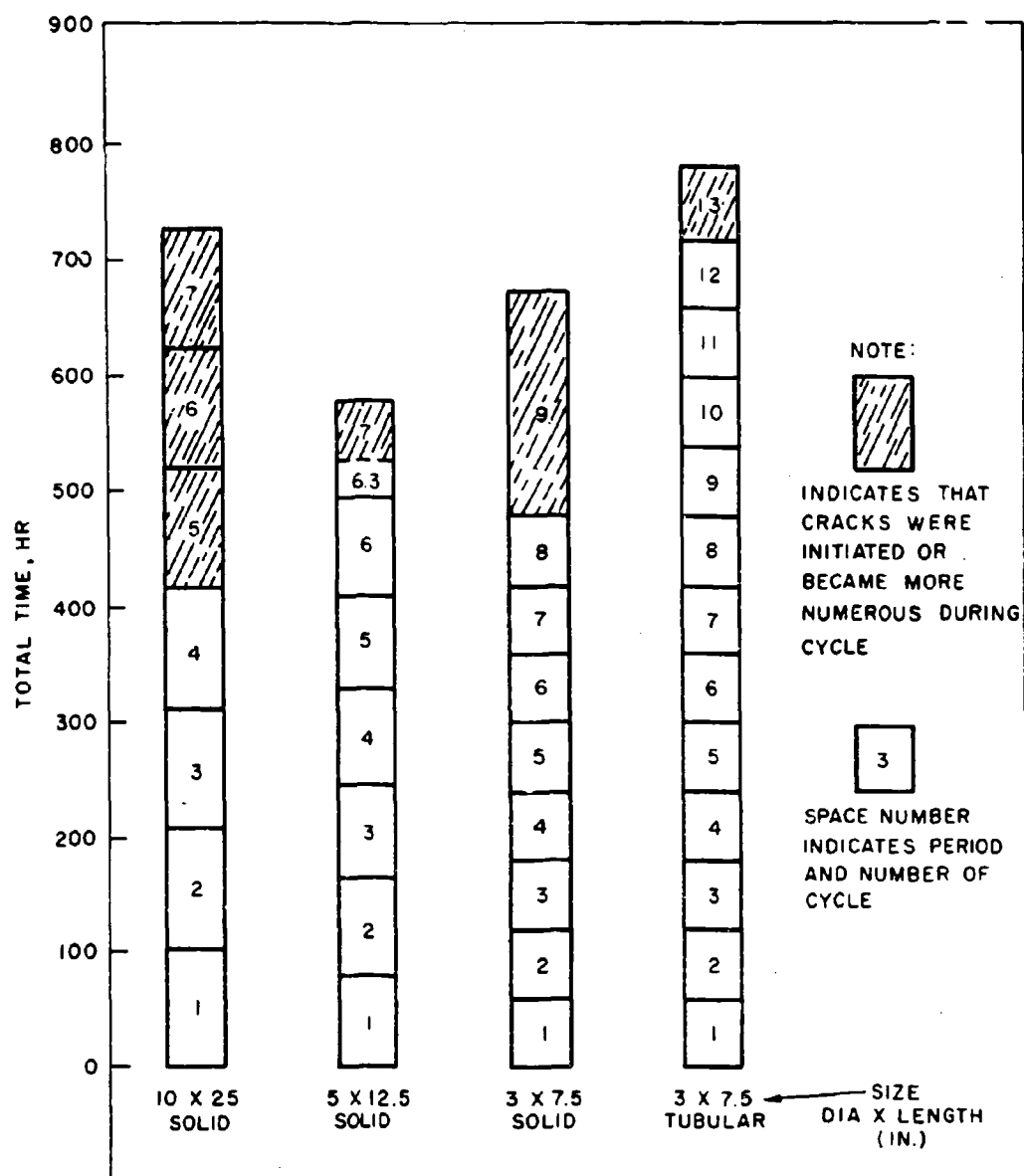FIG. 35. Isothermal Weight-Loss Studies on JPL Propellant.

55

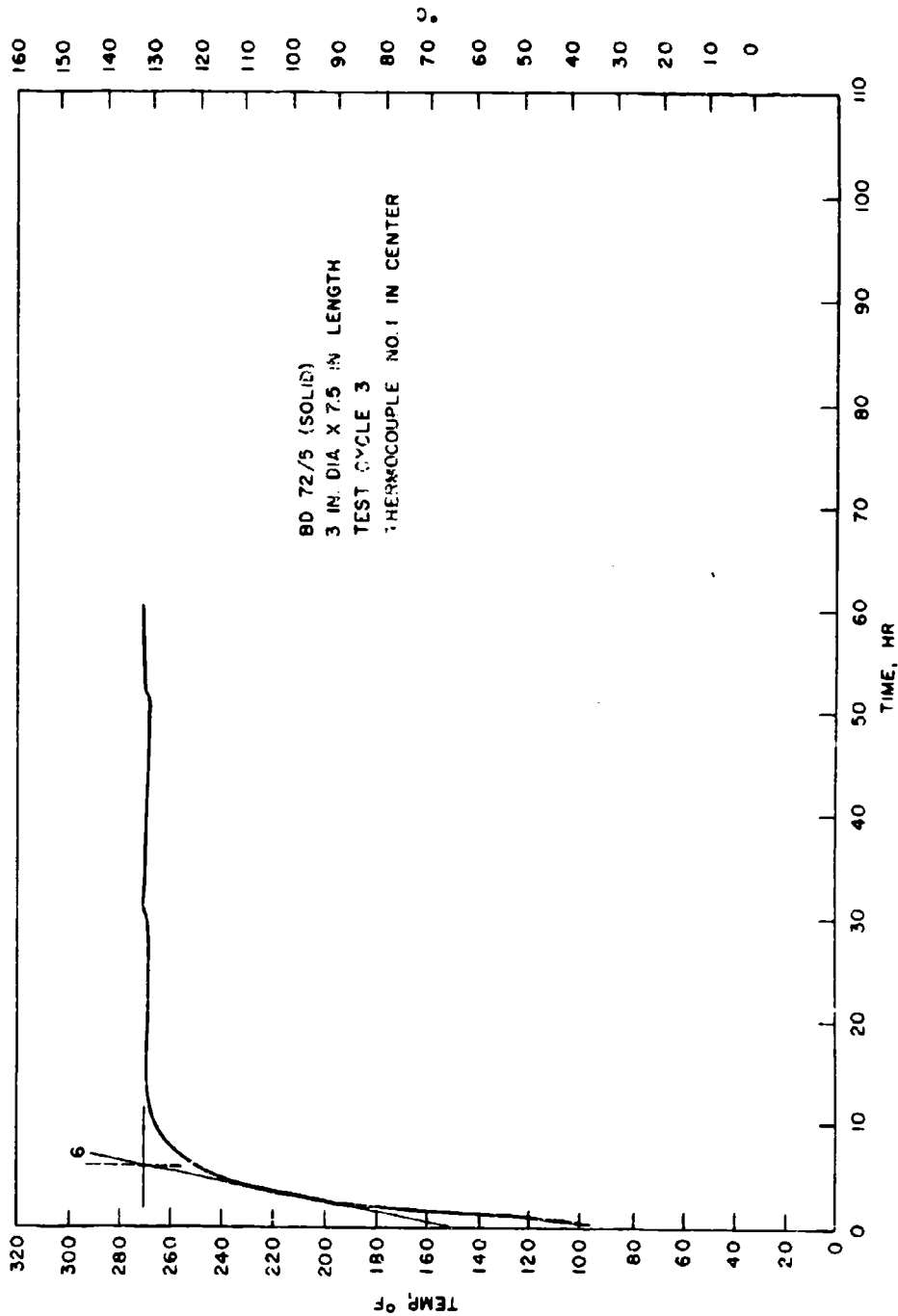FIG. 36. Results of Cycling Tests on JPL Propellant.

FIG. 37.   Determination of Correction Factor for 3-Inch Diameter JPL Propellant Charge.
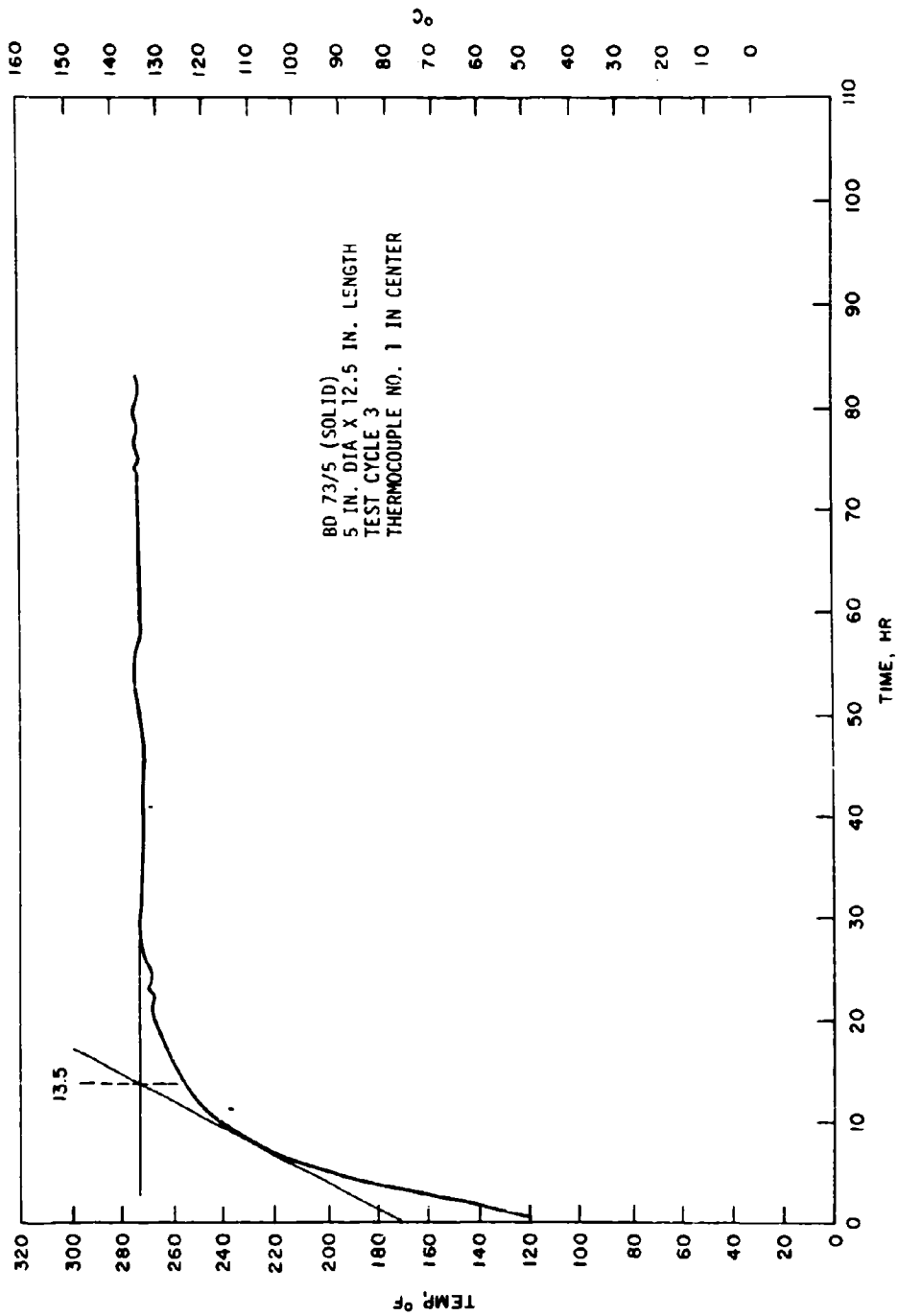
57

FIG. 38. Determination of Correction Factor for 5-Inch Diameter JPL Propellant Charge.
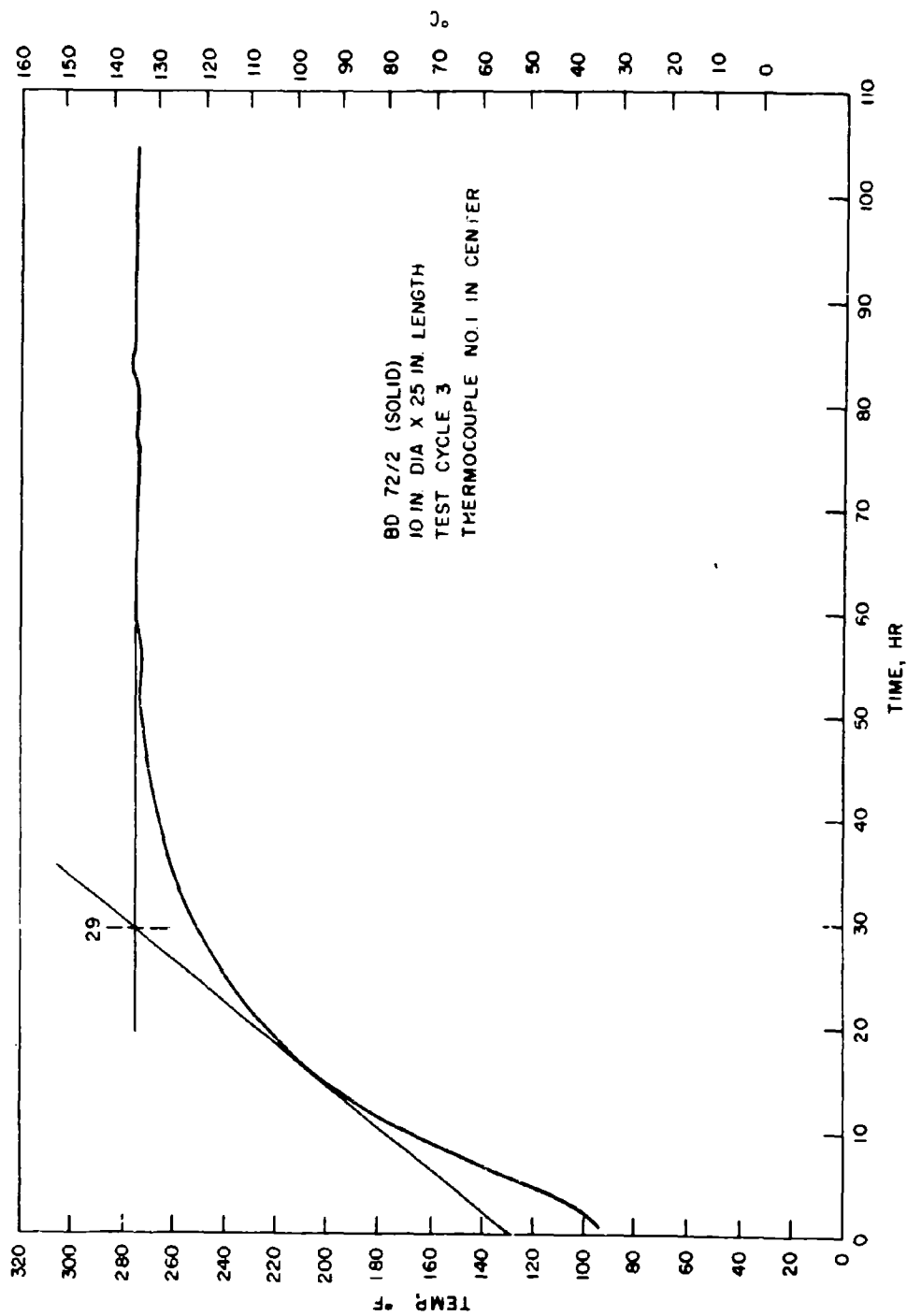
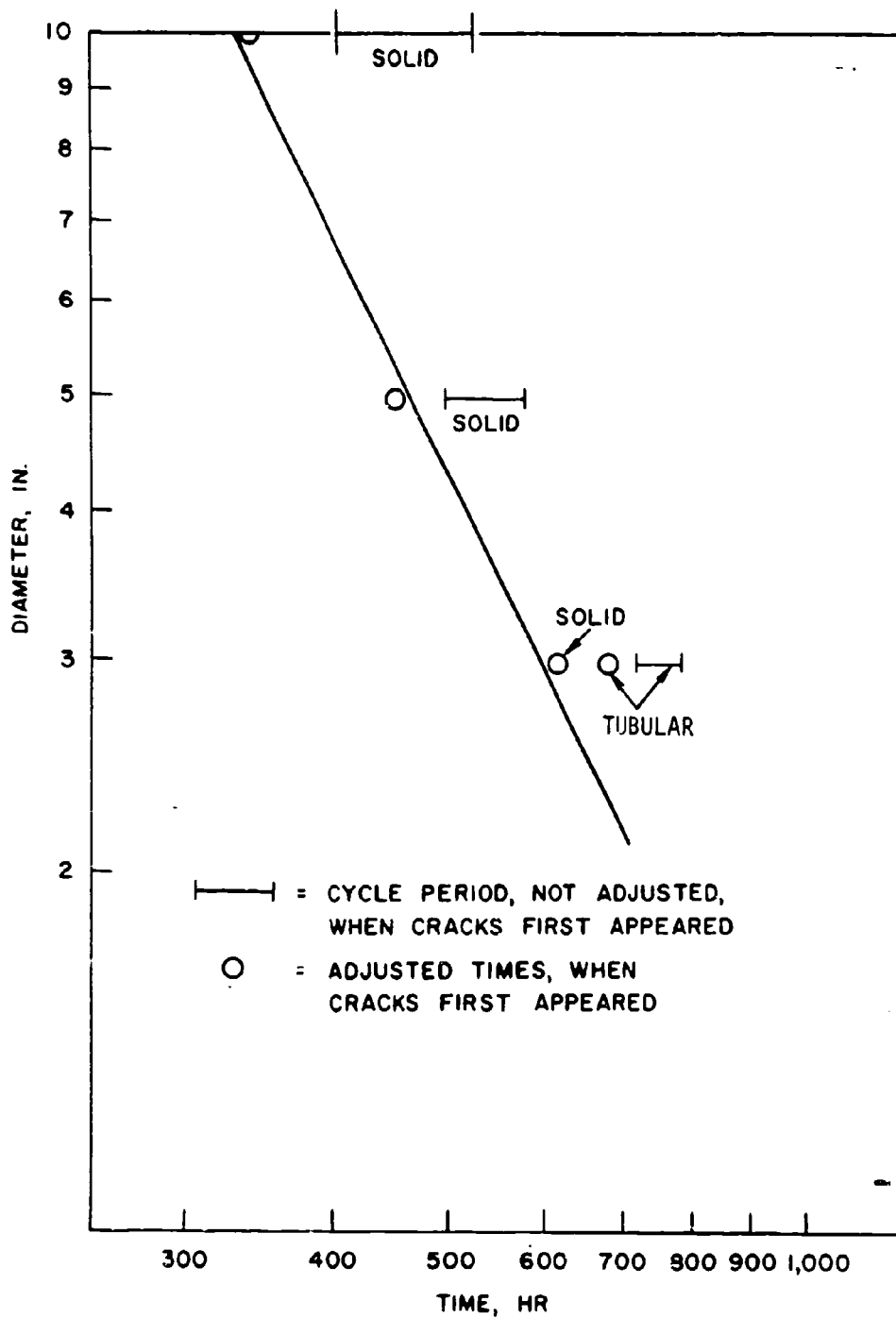FIG. 39. Determination of Correction Factor for 10-Inch Diameter JPL Propellant Charge.

BD 72/2 (SOLID)
10 IN DIA X 25 IN. LENGTH
TEST CYCLE 3
THERMOCOUPLE NO.1 IN CENTER

29

FIG. 40. First Appearance of Cracks During Cycling Tests on JPL Propellant Grains.

SIDE CROSS-SECTION

NOTE: NO.7 THERMOCOUPLE
LOCATED IN THE
GROUND

NOZZLE END-VIEW

SECTION A-A

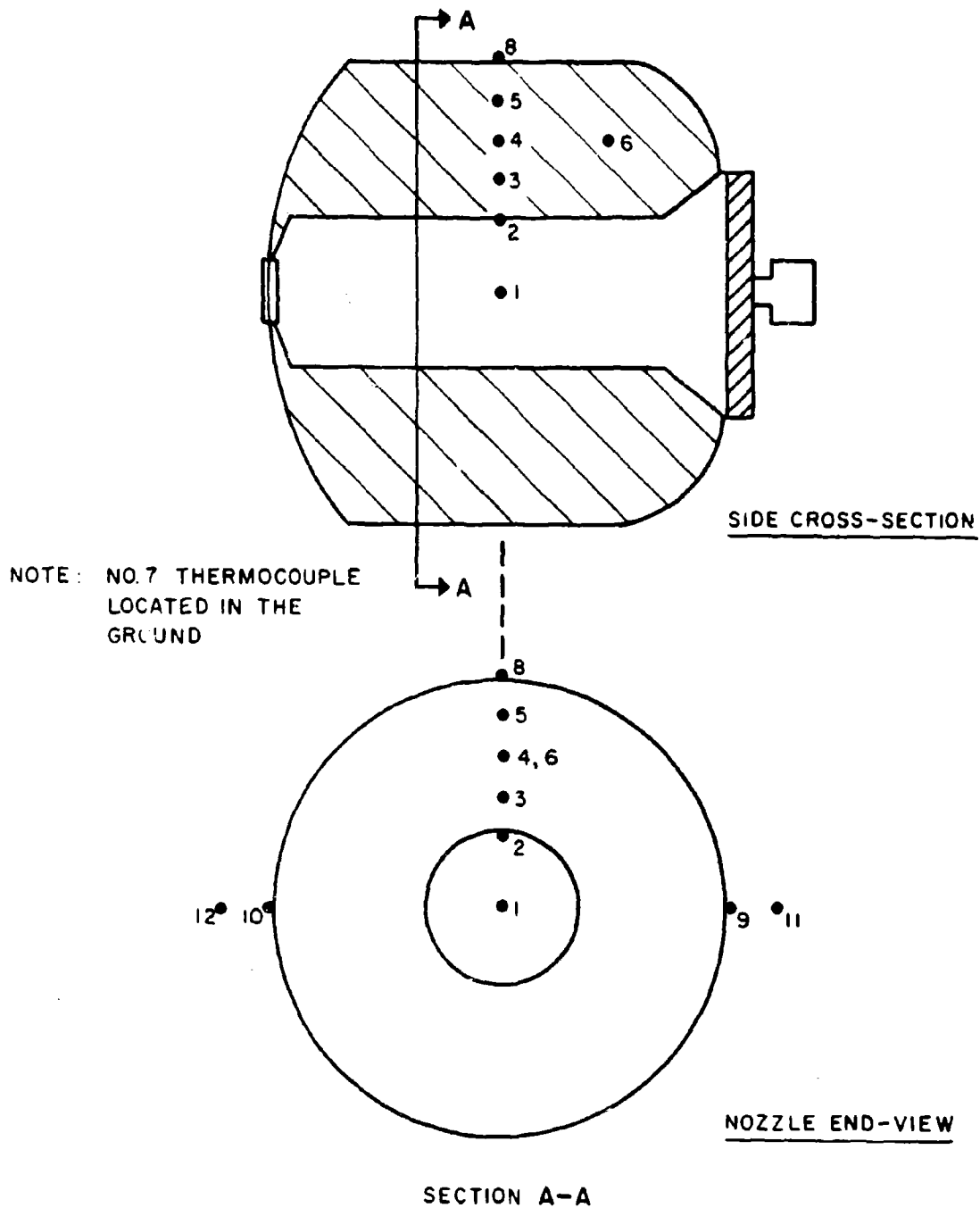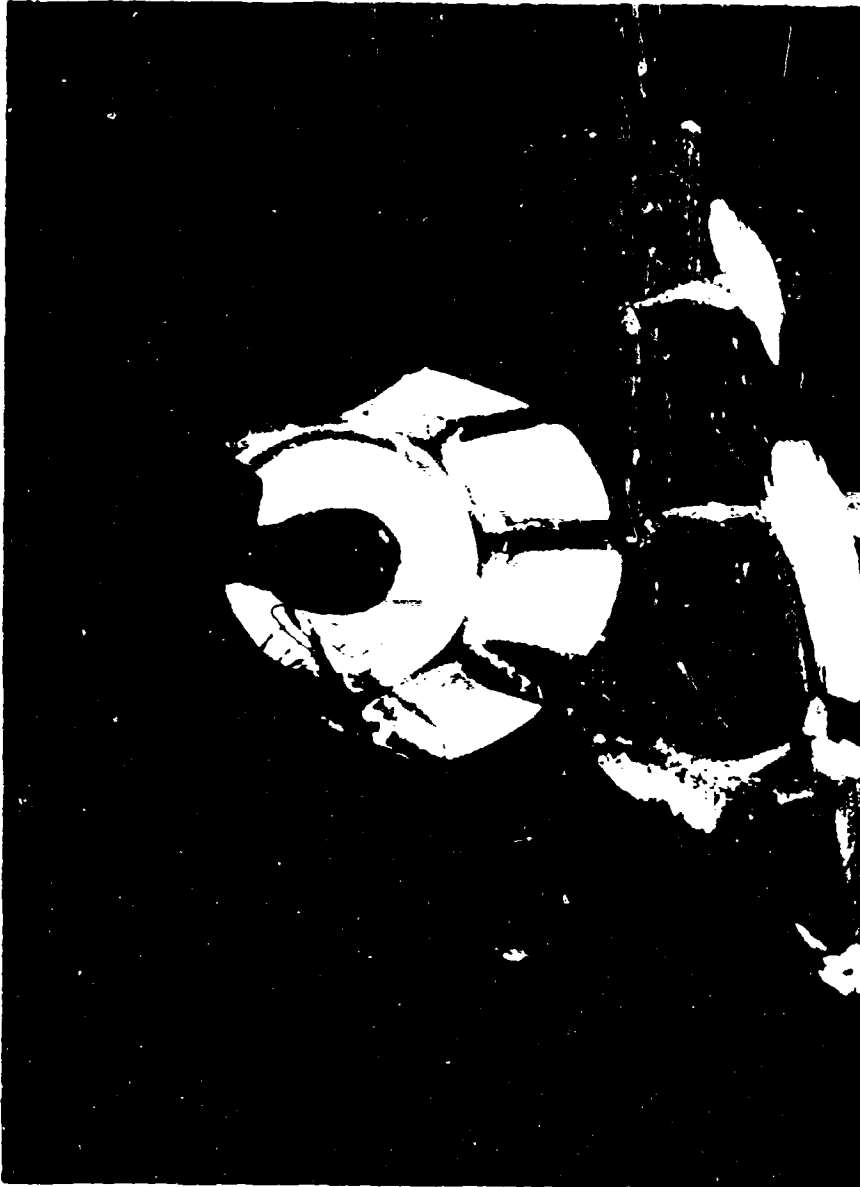FIG. 41. Location of Thermocouples in a 60-Pound, 12-Inch
Diameter Motor Used for Cycling Tests.

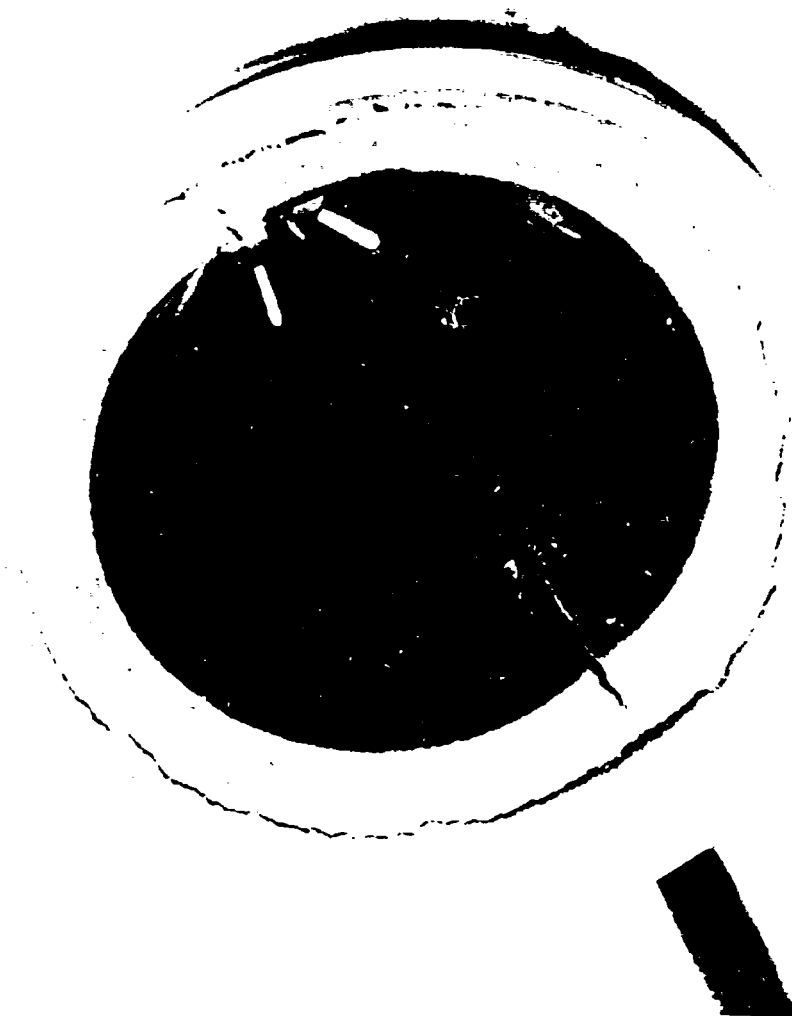FIG. 42. Nozzle-End View of a 60-Pound, 12-Inch Diameter Motor After First Test Cycle.

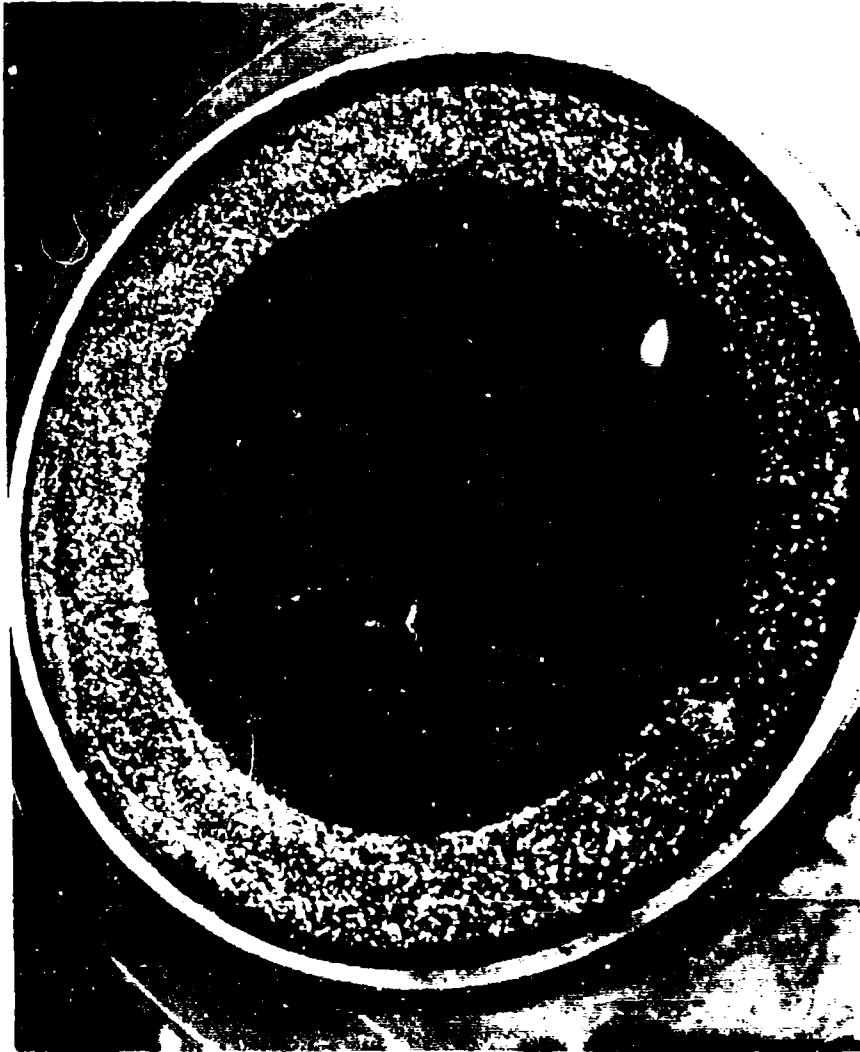LHI. 113718

LHL 113887

FIG. 43. Internal View of a 60-Pound, 12-Inch Diameter
Motor After First Test Cycle.

LHL 131030

FIG. 44. Nozzle-End View of a 60-Pound, 12-Inch
Diameter Motor After Second Test Cycle.

LHL 131031

FIG. 45.   Nozzle-End View of a 60-Pound, 12-Inch
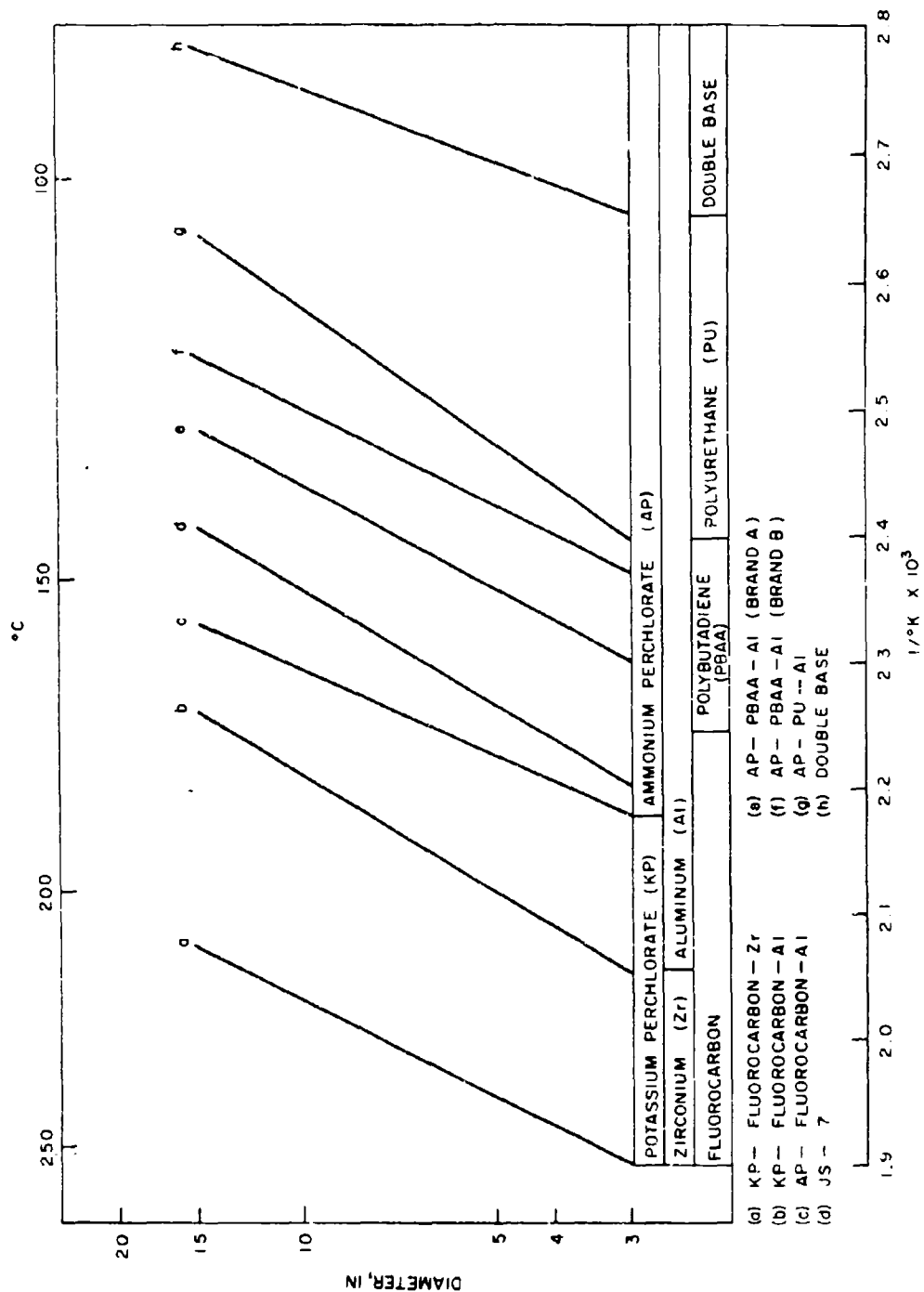Diameter Motor After Fourth Test Cycle.

FIG. 46. Temperature Ranges for Various Ingredients Used in Solid Propellants.

66

REFERENCES

1. Longwell, P. A. "Determination of Self-Heating Reaction Kinetics Data Applicable at Low Temperatures," Tech. Memo. 865. Aerojet-General Corporation (July 1965).

2. U. S. Naval Ordnance Test Station. Calculation of Critical Temperature and Time-to-Explosion for Propellants and Explosives, by P. A. Longwell, China Lake, Calif., NOTS, March 1961. (NAVWEPS Report 7646, NOTS TP 2663).

3. ------. The Thermal Decomposition Characteristics of Explosives (U), by C. D. Lind. China Lake, Calif., NOTS, February 1962. (NAVWEPS Report 7798, NOTS TP 2792), CONFIDENTIAL.

4. Zinn, J. and C. L. Mader. "Thermal Initiation of Explosives," J. APPL. PHYSICS, Vol. 31, No. 2 (1960), p. 323.

5. Zinn, J., and R. N. Rogers. "Thermal Initiation of Explosives," J. PHYS. CHEM., Vol. 66, (1961), p. 2646.

6. Kissinger, H. E. "Reaction Kinetics in Differential Thermal Analysis," ANAL. CHEM., Vol. 29 (November 1957), p. 1702.

7. Thompson, D. S., R. L. Reed, L. Weber, and B. S. Gottfried. "Differential Thermal Analysis and Reaction Kinetics," IND. ENG. CHEM. FUNDAMENTALS, Vol. 5, No. 2 (May 1966), p. 286.

8. U. S. Naval Ordnance Test Station. Predicting Propellant Safe-Life (U), by Jack M. Pakulak, Jr., China Lake, Calif., NOTS, 11 October 1961. (NAVWEPS Report 7775, NOTS TP 2756), CONFIDENTIAL.

9. Borchardt, H. J. and F. Daniels. J. AM. CHEM. SOC., Vol. 79, (January 1957), p. 41.

10. Reed, R. L., L. Weber, and B. S. Gottfried. "Differential Thermal Analysis and Reaction Kinetics," IND. ENG. CHEM. FUNDAMENTALS, Vol. 4, No. 1 (February 1965), p. 38.

NOMENCLATURE

A	Frequency factor, $\sec^{-1}$
AP	Ammonium perchlorate
a	Radius, cm
$\lvert A_t \rvert$	Remaining area of DTA peak
c	Heat capacity
C_o	Initial concentration
C_1	Concentration after a specific time at a specific temperature
d/D	Ratio, inside diameter/outside diameter
$\dfrac{dT}{dt}$	Heating rate at the surface of the grain, °C/sec
DTA	Differential thermal analysis
E	Activation energy, cal/mole
F	Function depending on geometry and the initial temperature
f	The fraction reacted
k	Specific rate constant, $\sec^{-1}$
L/D	Ratio, length/diameter
MAPO	Tri(methylaziridinyl) phosphine oxide
PBAA	Polybutadiene acrylic acid
Q	Heat of reaction, cal/g
R	Gas constant, 1.987 cal/(mole)(°K)
T	Absolute temperature
t	Time, seconds
T_1	Maximum surface temperature
T_c	The center temperature
t_e	Time to exotherm or deflagration, sec
TGA	Thermogravimetric analysis
T_m	Critical temperature, °K
T_{rp}	Absolute temperature of peak (°K) with respect to the reference temperature
ΔT	Differential temperature

68

w	Mass fraction unreacted at time, t
α	Thermal diffusivity, cm^2/sec
ϕ	Heating rate, °C/min
λ	Thermal conductivity, cal/(cm)(sec)(°K)
∇^2	Laplacian operator
ρ	Density, g/cm^3
δ	Shape factor
τ	Dimensionless time

DOCUMENT CONTROL DATA - R & D

Security classification of title, body of abstract and indexing annotation must be entered when the overall report is classified,

1. ORIGINATING ACTIVITY (Corporate author)	2a. REPORT SECURITY CLASSIFICATION
Naval Weapons Center	UNCLASSIFIED
China Lake, California 93555	2b. GROUP

3. REPORT TITLE

THERMAL ANALYSES STUDIES ON CANDIDATE SOLID JPL PROPELLANTS FOR HEAT STERILIZABLE MOTORS

4. DESCRIPTIVE NOTES (Type of report and inclusive dates)

5. AUTHOR(S) (First name, middle initial, last name)

Jack M. Pakulak, Jr. and Edward Kuletz

6. REPORT DATE	7a. TOTAL NO. OF PAGES	7b. NO. OF REFS
July 1970	70	10

8a. CONTRACT OR GRANT NO	9a. ORIGINATOR'S REPORT NUMBER(S)
JPL Purchase Order Nos. Z-351290 and	
b. PROJECT NO Z-351291	NWC TP 4258
c.	9b. OTHER REPORT NO(S) (Any other numbers that may be assigned this report)
d.	

10. DISTRIBUTION STATEMENT

THIS DOCUMENT IS SUBJECT TO SPECIAL EXPORT CONTROLS AND EACH TRANSMITTAL TO FOREIGN GOVERNMENTS OR FOREIGN NATIONALS MAY BE MADE ONLY WITH PRIOR APPROVAL OF THE NAVAL WEAPONS CENTER.

11. SUPPLEMENTARY NOTES	12. SPONSORING MILITARY ACTIVITY
	National Aeronautics & Space Administration
	Jet Propulsion Laboratory
	California Institute of Technology
	Pasadena, California

13. ABSTRACT

Times to deflagration of solid JPL propellant grains varying in size and geometry have been measured, and the results have been analyzed in light of the thermal explosion theory. In addition, laboratory-scale thermoanalytical techniques have been used to study the procedural chemical kinetics of the decomposition reactions of representative solid JPL propellants. The results of these studies indicate that, for the propellants considered, estimates of thermal deflagration times can be made on the basis of laboratory-scale experiments. The effects of sterilization heat cycling tests on solid JPL propellant grains varying in size and geometry have also been studied and the results are herein reported.

DD FORM 1473 (PAGE 1)
1 NOV 65

S/N 0101-807-6801

14 KEY WORDS	LINK A		LINK B		LINK C	
	ROLE	WT	ROLE	WT	ROLE	WT
Thermal Analysis						
Kinetic Studies						
Solid Propellants						
Heat Cycling						
Degradation						
Critical Temperature						
Cook-Off						